diated effects on the differentiation/proliferation of HSCs and monocyte-lineage cells by flow cytometric analysis. The number of GMP was much lower in apoE$^{-/-}$/BM-Agtr1$^{-/-}$ mice (34%, $P<0.05$), whereas HSCs and CMP did not differ between the 2 groups (Figure 1B). The expression level of CCR2 on monocyte-lineage cells was not impaired in Agtr1$^{-/-}$ mice (supplemental Figure II).

M-CSF–Induced Macrophage-Colony–Forming Activity Is Attenuated in BM Cells From AT_1-Deficient Mice

We first compared the numbers of HSCs, CMP, and GMP between Agtr1$^{+/+}$ and Agtr1$^{-/-}$ mice under steady-state condition without hypercholesterolemia. There was no difference between the 2 genotypes of mice, suggesting that the steady-state development of monocyte-lineage cells is relatively well preserved in Agtr1$^{-/-}$ mice (supplemental Figure IIIA, supplemental Table III). We next performed a macrophage-colony–forming assay to investigate whether the response to M-CSF is attenuated in BM cells from Agtr1$^{-/-}$ mice. Stimulation by M-CSF markedly increased the number of macrophage-colony units in BM cells from Agtr1$^{+/+}$ mice, which was remarkably diminished in BM cells from Agtr1$^{-/-}$ mice ($P<0.01$; supplemental Figure IIIB), suggesting that BM-AT_1 is crucially implicated in M-CSF–induced differentiation/proliferation of HSCs into monocyte-lineage cells.

M-CSF–Induced Differentiation From HSCs to Monocyte-Lineage Cells Is Suppressed in HSCs From AT_1-Deficient Mice

We examined the time course of differentiation of HSCs from Agtr1$^{+/+}$ mice into monocyte-lineage cells with or without M-CSF. Stimulation by M-CSF preferentially increased the number of promonocytes (CD11b^{high}Ly-6G^{low}) terminally differentiated from myeloid progenitor (MP: c-Kit$^+$Sca-1$^-$Lin$^-$; supplemental Figure IV).

We next compared the differentiation potential of HSCs between Agtr1$^{+/+}$ and Agtr1$^{-/-}$ mice (Figure 2). In the absence of M-CSF, the numbers of myeloid progenitors and promonocytes (CD11b^{high}Ly-6G^{low}) did not differ between the 2 genotypes. In contrast, stimulation by M-CSF markedly increased the number of promonocytes in both groups, whereas the extent was significantly attenuated in HSCs from Agtr1$^{-/-}$ mice (38%, $P<0.01$).

c-Fms Expression Is Inhibited in AT_1-Deficient Mice

The expression of M-CSF receptor c-Fms was examined by flow cytometry. Consistent with the previous finding,[16] the expression level of c-Fms (CD115) was gradually upregulated during the developmental stage from HSCs to promonocytes in Agtr1$^{+/+}$ mice, whereas the expression was severely decreased in all developmental stages in Agtr1$^{-/-}$ mice (Figure 3). The mRNA expression of c-Fms was also suppressed by 71% in Agtr1$^{-/-}$ mice ($P<0.05$; supplemental Figure V).

We also examined the effect of hypercholesterolemia on the c-Fms expression. Four-week Western diet feeding significantly increased the expression level of c-Fms (CD115) in all populations of HSCs, myeloid progenitors, and promonocytes compared with chow diet feeding (supplemental Figure VI). In contrast, BM-AT_1 expression was not affected by the Western diet feeding (supplemental Figure VII). These findings suggest that in the hypercholesterolemic setting, M-CSF–mediated growth of monocyte-lineage cells is enhanced by an increase in its receptor c-Fms expression.

Phosphorylation of PKC-δ and JAK2 Is Inhibited in Monocyte-Lineage Cells From AT_1-Deficient Mice

To investigate the effect of reduced c-Fms expression on its downstream signals, we examined the phosphorylation of PKC-δ and JAK2, which are known to be essential in M-CSF–induced differentiation/proliferation of monocyte-lineage cells.[17,18] In c-Kit$^+$ Lin$^-$ population including HSCs (c-Kit$^+$Sca-1$^+$Lin$^-$) and myeloid progenitors (c-Kit$^+$Sca-1$^-$Lin$^-$) from Agtr1$^{+/+}$ mice, the peak phosphorylation levels of PKC-δ and JAK2 were observed at 5 and 30 minutes after M-CSF stimulation, respectively (supplemental Figure VIIIA). The M-CSF–induced phosphorylation levels of PKC-δ and JAK2 at each time point were dramatically diminished in HSCs and myeloid progenitors from Agtr1$^{-/-}$ mice (80% and 75%, respectively, $P<0.01$; supplemental Figure VIIIB and VIIIC). These findings were also confirmed by Western blot analysis (supplemental Figure IX). We further examined the effect of PKC-δ inhibitor (rottlerin) or JAK2 inhibitor (AG490) on M-CSF–induced differentiation/proliferation of BM monocyte-lineage cells. Administration of rottlerin (10μmol/L) or AG490 (50μmol/L) into the culture medium completely diminished the M-CSF–induced increase in the number of promonocytes (supplemental Figure X).

The Expression of c-Fms on Promonocytes Is Not Affected by Ang II or ARB

We next studied how AT_1 signals regulate the c-Fms expression on HSCs/promonocytes. The result from the in vitro culture assay showed that 4-day treatment with Ang II (1 μmol/L) or ARB (10 μmol/L) did not affect the expression levels of c-Fms on HSCs, myeloid progenitors, and promonocytes (only data in promonocytes shown in Figure 4), and also did not affect M-CSF–mediated growth of HSCs, myeloid progenitors, and promonocytes (supplemental Figure XIA), suggesting that AT_1 receptor–mediated signals are not directly involved in the expression of c-Fms on HSCs and BM monocyte-lineage cells nor the differentiation from HSCs to promonocytes.

TNF-α Restores the Impaired Expression of c-Fms on Promonocytes From Agtr1$^{-/-}$ Mice

To further elucidate the mechanism by which Ang II regulates the expression of c-Fms, we next focused on the BM stromal cells (CD45$^-$CD34$^-$) other than hematopoietic-lineage cells, and examined the expression of TNF-α, because TNF-α has been reported to regulate the c-Fms expression in various cell types.[19,20] Interestingly, the expression level of TNF-α was extremely higher in the purified CD45$^-$CD34$^-$ BM stromal cells compared with that in promonocytes (supplemental Figure XIIA). Immunohistochemical analysis also showed that TNF-α–positive staining was mostly colocalized with BM stromal cells (supplemental Figure XIIB). Furthermore, we found that the number of

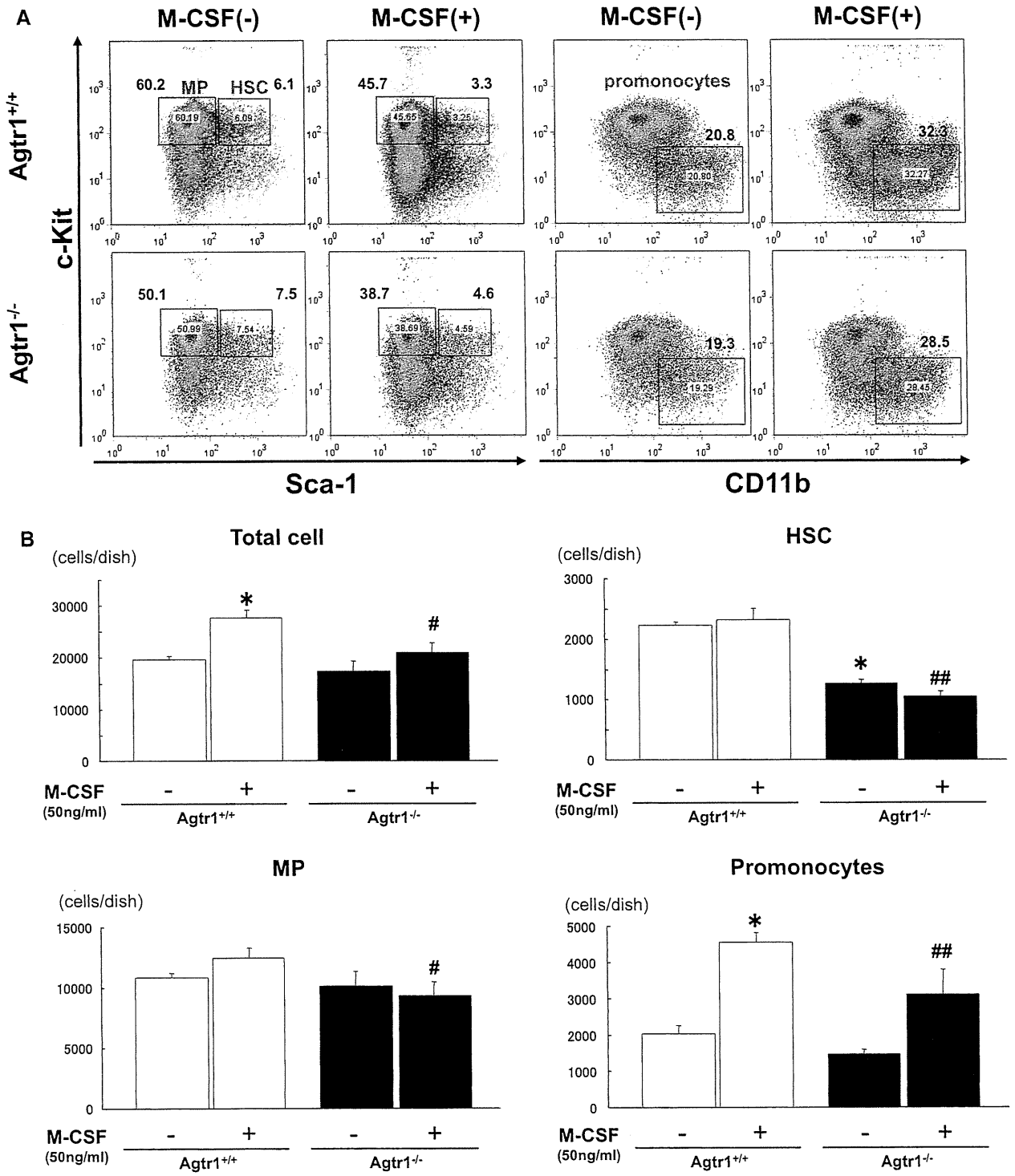

Figure 2. Inhibition of M-CSF–induced in vitro differentiation from HSCs into monocyte-lineage cells on ablation of marrow AT_1. A, Flow cytometry of c-Kit and Sca-1 expression in lineage-negative populations, and CD11b expression in c-Kit$^-$lineage-negative populations of HSCs from Agtr1$^{+/+}$ or Agtr1$^{-/-}$ mice cultured in the presence or absence of M-CSF (50 ng/mL) at day 4. B, Quantitative analysis showing an attenuated expansion of myeloid progenitors (MP:c-Kit$^+$Sca-1$^-$Lin$^-$) and promonocytes (CD11b^{high}Ly-6G^{low}) from Agtr1$^{-/-}$ mice after stimulation by M-CSF. HSCs indicates hematopoietic stem cells. Values are the mean±SE for at least 4 mice in each group. *P<0.01 vs Agtr1$^{+/+}$ cells cultured without M-CSF. #P<0.05, ##P<0.01 vs Agtr1$^{+/+}$ cells cultured with M-CSF.

CD45$^-$CD34$^-$ BM stromal cells was markedly diminished in Agtr1$^{-/-}$ mice compared with the Agtr1$^{+/+}$ mice (Figure 5A).

We further examined the effect of TNF-α on c-Fms expression in promoocytes from Agtr1$^{-/-}$ mice. Consistent with the previously reported data,[19,20] 4-day treatment with TNF-α (50 ng/mL) upregulated (65% versus control, P<0.01) the expression level of c-Fms in promonocytes from Agtr1$^{+/+}$ mice (Figure 4). Interestingly, the similar extent of

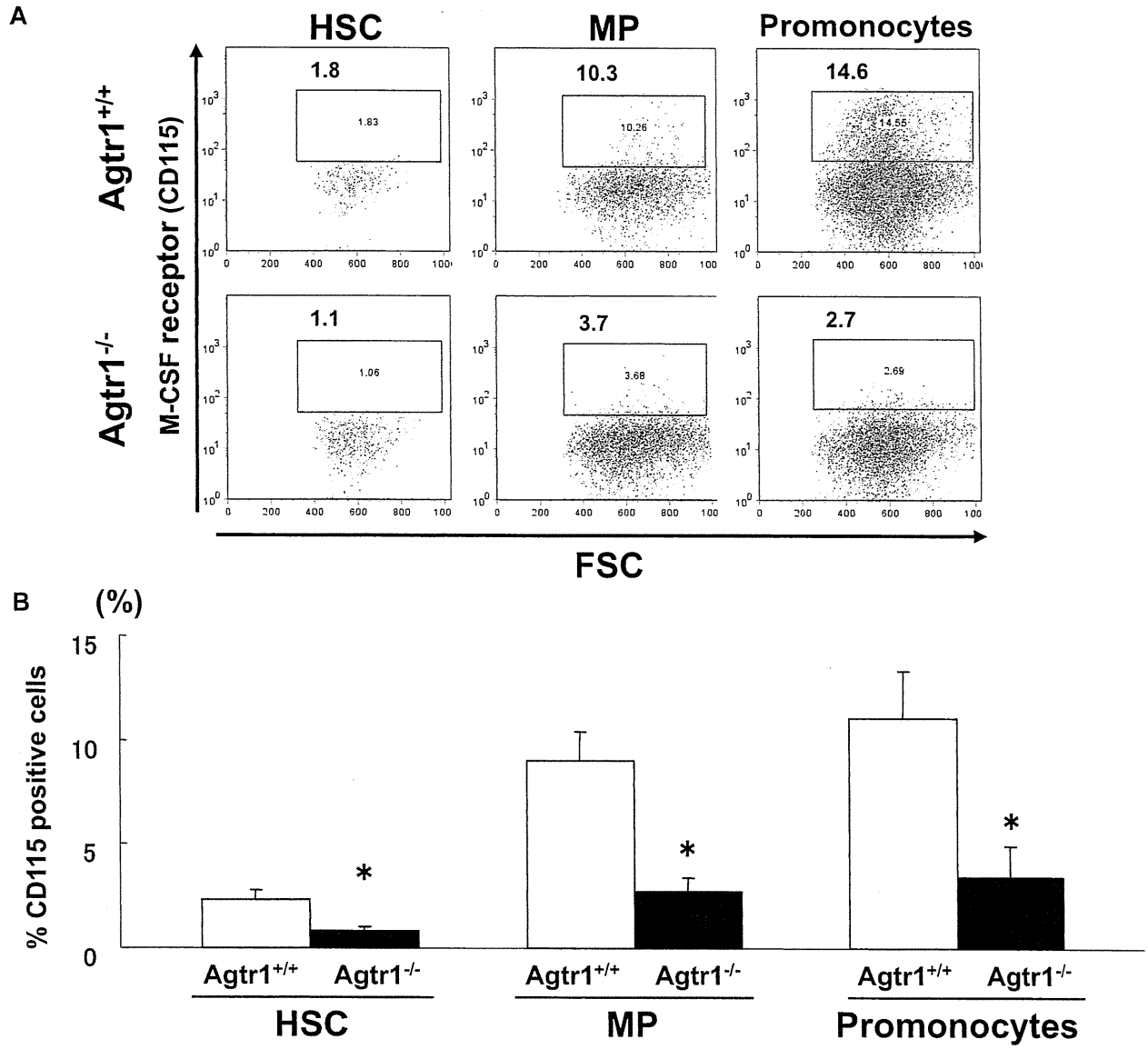

Figure 3. Inhibition of M-CSF receptor expression on ablation of marrow AT_1. A, Flow cytometry for c-Fms expression in HSCs, myeloid progenitors (MP:c-Kit$^+$Sca-1$^-$Lin$^-$), and promonocytes (CD11b^{high}Ly-6G^{low}) from Agtr1$^{+/+}$ and Agtr1$^{-/-}$ mice under steady-state condition without hypercholesterolemia. B, Quantitative analysis showing a significant inhibition of c-Fms expression in each fraction. Values are the mean±SE for at least 4 mice in each group. *$P<0.05$ vs Agtr1$^{+/+}$.

TNF-α–mediated induction of c-Fms was also observed in promonocytes from Agtr1$^{-/-}$ mice (Figure 4), indicating that TNF-α–mediated expression of c-Fms in HSCs and promonocytes is not impaired by AT_1 deficiency.

AT_1 Signals Regulate Growth of BM Stromal Cells and TNF-α Expression

The effects of AT_1 deficiency and ARB on the number of BM stromal cells and their expression of TNF-α were studied. Real-time PCR analysis showed that AT_1 mRNA expression is detectable in myeloid progenitors, promonocytes, and BM CD45$^-$CD34$^-$ stromal cells, whereas no significant expression is observed in HSCs (supplemental Figure XIII). One-week administration of ARB (Olmesartan: 3 mg/kg/d) into the wild-type mice profoundly reduced the percentage fraction of BM stromal cells, the extent of which was similar to that in Agtr1$^{-/-}$ mice (Figure 5A). Furthermore, ARB treatment significantly decreased the expression level of TNF-α mRNA in BM stromal cells (Figure 5C). Considering that Ang II did not affect the c-Fms expression (Figure 4) or the proliferation (supplemental Figure XIA) of HSCs, myeloid progenitors, and promonocytes, it is likely that the target of ARB is BM stromal cells, and Ang II directly regulates their growth and TNF-α synthesis/release, leading to the modulation of c-Fms expression on BM monocyte-lineage cells in a paracrine fashion.

ARB Reduces Atherosclerosis Accompanied by a Reduction of Monocyte-Lineage Cells Without Affecting Serum M-CSF Levels

We studied the effect of ARB on monocyte-lineage development in apoE$^{-/-}$ mice fed a Western diet. The atherosclerotic

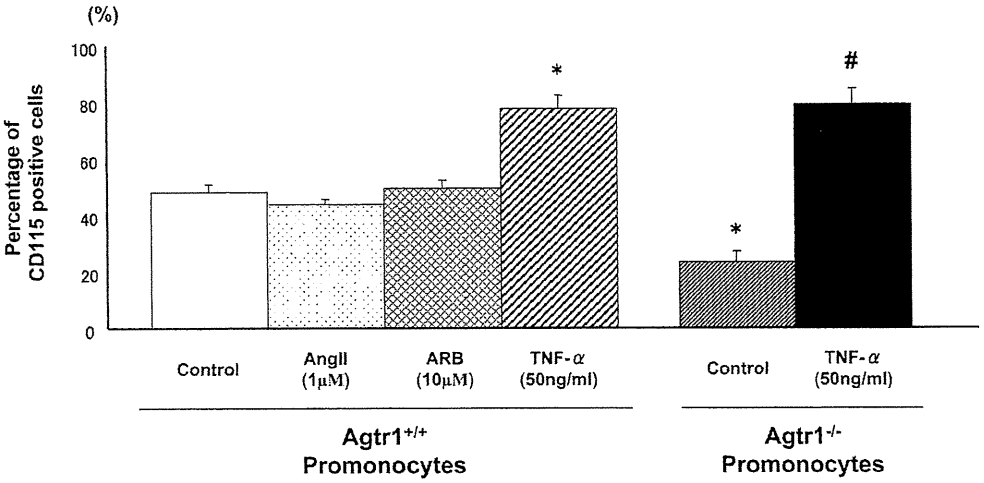

Figure 4. c-Fms expression on promonocytes is not affected by Ang II or ARB but augmented by TNF-α. Hematopoietic stem cells (HSCs) were isolated from Agtr1$^{+/+}$ mice and cultured with Ang II (1 μmol/L) or ARB (10 μmol/L) for 4 days. The expression levels of c-Fms on HSCs, myeloid progenitors, and promonocytes (only data in promonocytes were shown) were not affected by Ang II or ARB treatment. In contrast, treatment with TNF-α (50 ng/mL) upregulated c-Fms expression on promonocytes. Whereas the c-Fms expression was significantly impaired in promonocytes from Agtr1$^{-/-}$ mice, the similar extent of TNF-α–mediated induction are observed. Values are the mean±SE for at least 4 mice in each group. *P<0.05 vs promonocytes from Agtr1$^{+/+}$ mice. #P<0.05 vs promonocytes from Agtr1$^{-/-}$ mice.

lesion area showed a significant reduction in ARB-treated mice compared with hydralazine- and saline-treated mice (supplemental Figure XIVA). Whereas the number of myeloid progenitors was significantly increased by 4-week Western diet feeding, it was completely reduced in ARB-treated mice (supplemental Figure XIVB), consistent with the results from BM chimeric mice. Furthermore, the frequency of circulating monocytes (CD11b^{high}Ly-6G^{low}Ly-6C^{high}) in saline- and hydralazine-treated mice was completely diminished in ARB-treated mice (supplemental Figure XIVB). The serum M-CSF concentration was significantly elevated by 4-week Western diet feeding but was not suppressed by ARB treatment (supplemental Figure XIVC). These findings suggest that the decreased number of monocyte-lineage cells in ARB-treated hypercholesterolemia mice is not attributable to a decrease in serum M-CSF levels but to the direct actions of ARB on BM cells.

Discussion

The present study demonstrated that Ang II affects the expression profile of the M-CSF receptor c-Fms on HSCs and monocyte-lineage cells through BM stromal cell–derived TNF-α, and thereby regulates M-CSF–mediated differentiation/proliferation of BM monocyte-lineage cells followed by the mobilization of monocytes, which contributes to the AT_1-mediated proatherogenic actions. These findings provide novel information on the BM renin–angiotensin system and a unique opportunity to develop therapeutic strategies targeting BM stem cells for the prevention of atherosclerotic cardiovascular disease.

In contrast with Ang II–induced atherosclerosis, the role of BM-AT_1 on hypercholesterolemia-induced atherosclerosis is controversial. Fukuda et al[8] demonstrated that apoE$^{-/-}$ mice repopulated with Agtr1$^{-/-}$ marrow showed a modest but significant reduction of atherosclerotic lesion development, whereas ablation of BM-AT_1 receptor in LDLr$^{-/-}$ mice had no effect on atherosclerosis,[7,21] suggesting that the different models used may differ in their consequence of BM-AT_1 on atherosclerosis. Indeed, Strawn et al[12] demonstrated that native LDL significantly upregulated AT_1 receptor expression on CD34$^+$ cells, which was completely diminished by treatment with a neutralizing LDL receptor antibody, suggesting that hypercholesterolemia-induced expression of AT_1 receptor is comparatively higher in apoE$^{-/-}$ mice than LDLr$^{-/-}$ mice. In addition, Daugherty et al[2] demonstrated that hypercholesterolemia extensively increased the plasma Ang II concentration in LDLr$^{-/-}$ mice, which was completely abolished in Agtr1$^{-/-}$ mice. Taken together, it is quite likely that BM-AT_1 receptor activation is more implicated in the hypercholesterolemia-induced atherosclerosis in apoE$^{-/-}$ mice rather than LDLr$^{-/-}$ mice.

BM stem cells are primed for multilineage gene expression and can differentiate into all types of blood cells.[14,15] M-CSF is the principal regulator of proliferation and terminal differentiation of monocyte-lineage cells.[22] We found that M-CSF–induced colony forming activity was dramatically attenuated in BM cells from Agtr1$^{-/-}$ mice, and that in vitro differentiation of HSCs from Agtr1$^{-/-}$ mice was significantly reduced in the presence of M-CSF. We further demonstrated that M-CSF receptor c-Fms expression and its downstream signaling were impaired. In hypercholesterolemia, activated endothelial cells, vascular smooth muscle cells, and inflammatory leukocytes have been shown to secrete a variety of cytokines, chemokines, and growth factors, including M-CSF.[23] In this study, we showed that serum M-CSF levels were significantly elevated in apoE$^{-/-}$ mice fed a Western diet (supplemental Figure XIVC). Accordingly, Ang II–mediated action in the differentiation/proliferation of monocyte-lineage cells is considered to be more augmented in various pathological conditions[24,25] as well as atherosclerosis, in which serum M-CSF levels were elevated.

The M-CSF receptor c-Fms is encoded by the *c-fms* protooncogene,[26] whose expression is predominantly regulated by the transcription factor Pu.1.[27] Agtr1$^{-/-}$ mice do not show any phenotype of low growth rate, tooth deficiency, severe osteopetrosis, reduced bone marrow cellularity, or

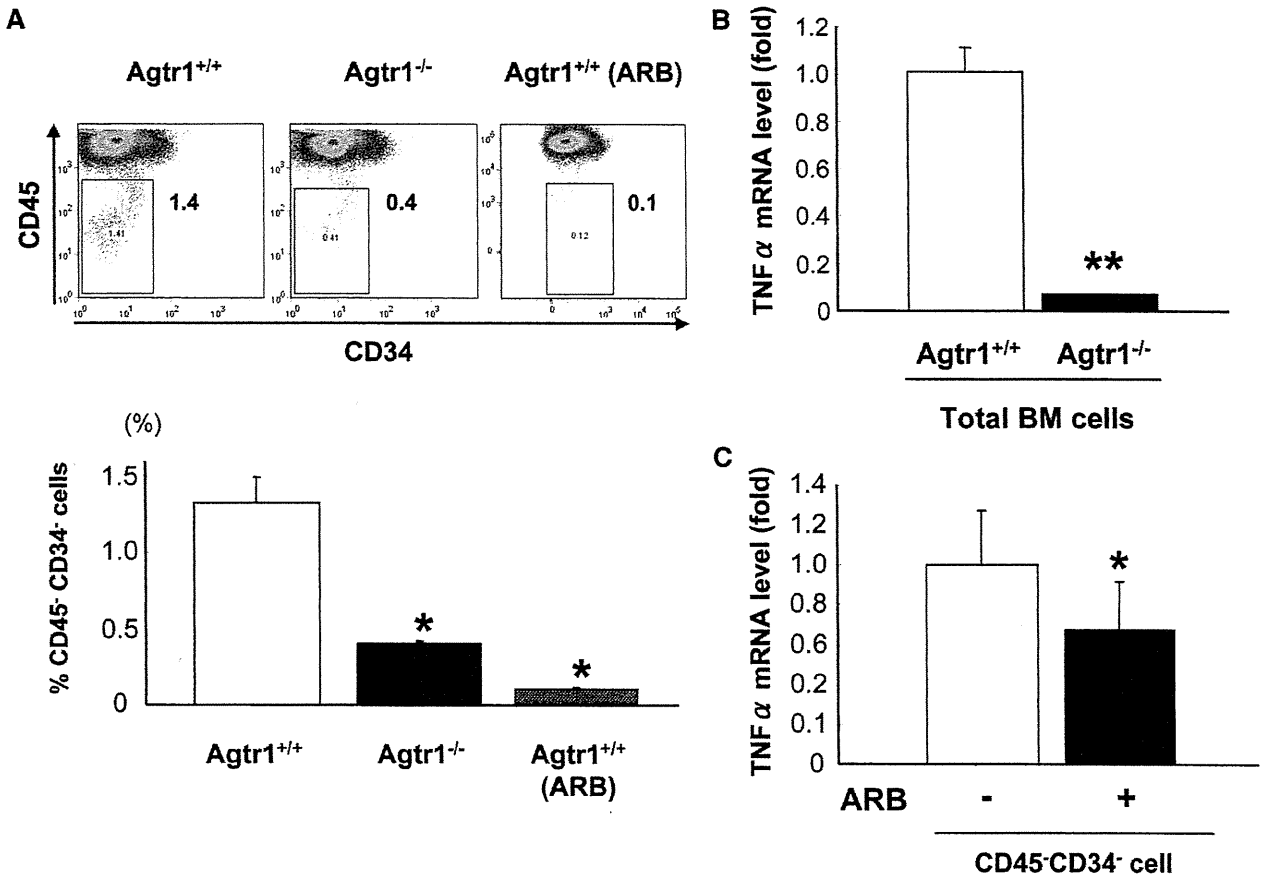

Figure 5. AT_1 signals regulate growth of BM stromal cells and TNF-α expression. A, The percentage fraction of BM $CD45^-CD34^-$ cells was reduced in $Agtr1^{-/-}$ mice. One-week administration of ARB (Olmesartan: 3 mg/kg/d) into $Agtr1^{+/+}$ mice also reduced the percentage fraction of BM $CD45^-CD34^-$ cells. Values are the mean±SE for at least 4 mice in each group. *$P<0.05$ vs saline-treated $Agtr1^{+/+}$ mice. B, Real-time PCR analysis showing the reduced expression of TNF-α in total BM cells from $Agtr1^{-/-}$ mice. C, One-week treatment with ARB (Olmesartan: 3 mg/kg/d) on $Agtr1^{+/+}$ mice significantly decreased the expression level of TNF-α mRNA in BM stromal cells. Total RNA was isolated from the same cell numbers of BM cells (B) or $CD45^-CD34^-$ cells (C), and TNF-α mRNA levels was shown as values relative to the control. Values are the mean±SE for at least 4 mice in each group. *$P<0.05$, **$P<0.01$ vs control $Agtr1^{+/+}$ mice.

depletion of circulating monocytes, all of which were observed in $Csf1r^{-/-}$ mice,[28] in which the c-Fms gene is genetically disrupted. Likewise, $Agtr1^{-/-}$ mice do not show any of the phenotypes observed in $PU.1^{-/-}$ mice.[29] TNF-α directly stimulates BM blood osteoclast precursor genesis by enhancing c-Fms expression.[19,20] TNF-α increased the expression level of c-Fms on promonocytes from $Agtr1^{-/-}$ mice to the same extent as $Agtr1^{+/+}$ mice (Figure 4), suggesting that TNF-α–mediated expression of c-Fms is not impaired by AT_1 deficiency. Given the reduced expression of TNF-α in BM cells from $Agtr1^{-/-}$ mice (Figure 5B), it is conceivable that decreased expression of c-Fms in monocyte-lineage cells from $Agtr1^{-/-}$ mice is primarily attributable to the impaired TNF-α–mediated actions.

Bone marrow niche plays an important role in the differentiation and proliferation of HSCs, in which BM stromal cells and mesenchymal stem cells (MSCs) regulate localization, self-renewal, and differentiation of HSCs through the secretion of cytokines and growth factor, cell-to-cell interactions, and the influence of extracellular matrix proteins.[30] Recently, Matsushita et al reported that BM-MSCs expressed AT_1 receptor and secreted Ang II.[31] BM stromal cells and BM-MSCs have been reported to secrete TNF-α as well as M-CSF.[32] Our present study demonstrates that TNF-α derived from BM stromal cells upregulates the c-Fms expression on HSCs and BM monocyte-lineage cells, and that AT_1 deficiency is indirectly involved in the regulation of c-Fms expression by inhibiting the proliferation of BM stromal cells. Considering that ARB treatment of the wild-type mice inhibits the proliferation of BM stromal cells (Figure 5), and that AT_1 signals activate ERK1/2 and Akt pathways in mesenchymal stem cells,[33] it is likely that Ang II plays an important role in the proliferation of BM stromal stem cells rather than HSCs. In fact, the mRNA expression level of AT_1 is much higher in BM stromal cells, whereas no expression was detected in HSCs (supplemental Figure XIII). Further studies will be needed to elucidate how Ang II differentially regulates the proliferation and differentiation of BM stem cells.

ARB treatment significantly attenuated macrophage-colony-forming activity in a dose-dependent manner (supplemental Figure XIB). Ang II has been shown to augment the number of macrophage-colony forming units.[5] In contrast with these findings, neither Ang II nor ARB treatment affected the M-CSF–induced differentiation of monocyte-

lineage cells in vitro culture assay. Colony forming unit assays were performed using total BM cells that include nonhematopoietic lineage cells such as BM stromal cells and BM-MSCs. The discrepant result from in vitro culture assay seems to be attributable to the effects of Ang II or ARB on BM stromal cells and BM-MSCs. Thus, the target of ARB is BM stromal cells, and Ang II directly regulates their growth and TNF-α synthesis/release, leading to the modulation of c-Fms expression on BM monocyte-lineage cells.

In conclusion, our findings demonstrate that Ang II promotes the M-CSF–mediated differentiation/proliferation of BM monocyte-lineage cells through TNF-α–mediated up-regulation of c-Fms expression, and that the TNF-α is mainly derived from BM stromal cells growth-controlled by Ang II and specifically regulates the c-Fms expression on monocyte-lineage cells, thus leading to the increased numbers of circulating monocytes that modulate AT_1-mediated proatherogenic activities.

Acknowledgments

We thank Prof Todo T. and Kobayashi J. and the Radiation Biology Center Kyoto University (H18-17) for assistance with bone marrow transplantation.

Sources of Funding

This work was supported by a grant from the Ministry of Education, Culture, Sports, Science, and Technology of Japan (00240036).

Disclosures

None.

References

1. Daugherty A, Manning MW, Cassis LA. Angiotensin II promotes atherosclerotic lesions and aneurysms in apolipoprotein E–deficient mice. *J Clin Invest.* 2000;105:1605–1612.
2. Daugherty A, Rateri DL, Lu H, Inagami T, Cassis LA. Hypercholesterolemia stimulates angiotensin peptide synthesis and contributes to atherosclerosis through the AT_{1A} receptor. *Circulation.* 2004;110:3849–3857.
3. Wassmann S, Czech T, van Eickels M, Fleming I, Böhm M, Nickenig G. Inhibition of diet-induced atherosclerosis and endothelial dysfunction in apolipoprotein E/angiotensin II type 1A receptor double-knockout mice. *Circulation.* 2004;110:3062–3067.
4. Brasier AR, Recinos III A, Eledrisi MS. Vascular inflammation and the renin-angiotensin system. *Arterioscler Thromb Vasc Biol.* 2002;22:1257–1266.
5. Rodgers KE, Xiong S, Steer R, diZerega GS. Effect of angiotensin II on hematopoietic progenitor cell proliferation. *Stem Cells.* 2000;18:287–294.
6. Petnehazy T, Stokes KY, Wood KC, Russell J, Granger DN. Role of blood cell-associated AT1 receptors in the microvascular responses to hypercholesterolemia. *Arterioscler Thromb Vasc Biol.* 2006;26:313–318.
7. Cassis LA, Rateri DL, Lu H, Daugherty A. Bone marrow transplantation reveals that recipient AT1a receptors are required to initiate angiotensin II-induced atherosclerosis and aneurysms. *Arterioscler Thromb Vasc Biol.* 2007;27:380–386.
8. Fukuda D, Sata M, Ishizaka N, Nagai R. Critical role of bone marrow Angiotensin II type 1 receptor in the pathogenesis of atherosclerosis in apolipoprotein E-deficient mice. *Arterioscler Thromb Vasc Biol.* 2008;28:90–96.
9. Østerud B, Bjorklid E. Role of monocytes in atherogenesis. *Physiol Rev.* 2003;83:1069–1112.
10. Feldman DL, Mogelesky TC, Liptak BF, Gerrity RG. Leukocytosis in rabbits with diet-induced atherosclerosis. *Arterioscler Thromb.* 1991;11:985–994.
11. Swirski FK, Libby P, Aikawa E, Alcaide P, Luscinskas FW, Weissleder R, Pittet MJ. Ly-$6C^{hi}$ monocytes dominate hypercholesterolemia-associated monocytosis and give rise to macrophages in atheromata. *J Clin Invest.* 2007;117:195–205.
12. Strawn WB, Ferrario CM. Angiotensin II AT1 receptor blockade normalized CD11b+ monocyte production in bone marrow of hypercholesterolemic monkeys. *Atherosclerosis.* 2008;196:624–632.
13. Urao N, Okigaki M, Yamada H, Aadachi Y, Matsuno K, Matsui A, Matsunaga S, Tateishi K, Nomura T, Takahashi T, Tatsumi T, Matsubara H. Erythropoietin-mobilized endothelial progenitors enhance reendothelialization via Akt-endothelial nitric oxide synthase activation and prevent neointimal hyperplasia. *Circ Res.* 2006;98:1405–1413.
14. Iwasaki H, Akashi K. Hematopoietic developmental pathway: on cellular basis. *Oncogene.* 2007;26:6687–6696.
15. Fogg DK, Sibon C, Miled C, Jung S, Aucouturier P, Littman DR, Cumano A, Geissmann F. A clonogenic bone marrow progenitor specific for macrophages and dendritic cells. *Science.* 2006;311:83–87.
16. Tagoh H, Himes R, Clarke D, Leenen PJM, Riggs AD, Hume D, Bonifer C. Transcription factor complex formation and chromatin fine structure alterations at the murine c-fms (CSF-1 receptor) locus during maturation of myeloid precursor cells. *Genes Dev.* 2002;16:1721–1737.
17. Baker SJ, Rane SG, Reddy EP. Hematopoietic cytokine receptor signaling. *Oncogene.* 2007;26:6724–6737.
18. Junttila I, Bourette RP, Rohrschneider LR, Silvennoinen O. M-CSF induced differentiation of myeloid precursor cells involves activation of PKC-δ and expression of Pkare. *J Leukoc Biol.* 2003;73:281–288.
19. Favot P, Yue X, Hume DA. Regulation of the c-fms promoter in murine tumor cell lines. *Oncogene.* 1995;11:1371–1381.
20. Yao Z, Li P, zhang Q, Schwarz EM, Keng P, Arbini A, Boyce B, Xing L. Tumor necrosis factor-α increase circulating osteoclast precursor numbers by promoting their proliferation and differentiation in the bone marrow through up-regulation of c-Fms expression. *J Biol Chem.* 2006;281:11846–11855.
21. Lu H, Rateri DL, Feldman DL, Charnigo Jr RJ, Fukamizu A, Ishida J, Oesterling Eg, Cassis LA, Daugherty A. Renin inhibition reduces hypercholesterolemia-induced atherosclerosis in mice. *J Clin Invest.* 2008;118:984–993.
22. Scott EW, Simon MC, Anastasi J, Singh H. Requirement of transcription factor PU. 1 in the development of multiple hematopoietic lineages. *Science.* 1994;265:1573–1577.
23. Chitu V, Stanley ER. Colony-stimulating factor-1 in immunity and inflammation. *Curr Opin Immunol.* 2006;18:39–48.
24. Davis TA, Lennon G. Mice with a regenerative wound healing capacity and an SLE autoimmune phenotype contain elevated numbers of circulating and marrow-derived macrophage progenitor cells. *Blood Cells Mol Dis.* 2005;34:17–25.
25. Campbell IK, Rich MJ, Bischof RJ, Hamilton JA. The colony-stimulating factor expression and collagen-induced arthritis: exacerbation of disease by M-CSF and G-CSF and requirement for endogenous M-CSF. *J Leukoc Biol.* 2000;68:144–150.
26. Hume DA, Yue X, Ross IL, Favot P, Lichanska A, Ostrowski MC. Regulation of CSF-1 receptor expression. *Mol Reprod Dev.* 1997;46:46–53.
27. Celada A, Borras FE, Soler C, Lloberas J, Klemsz M, Beveren C, McKercher S, Maki RA. The transcription factor PU. 1 is involved in macrophage proliferation. *J Exp Med.* 1996;184:61–69.
28. Dai M, Ryan GR, Hapel AJ, Dominguez MG, Russell RG, Kapp S, Sylvestre V, Stanley ER. Targeted disruption of the mouse colony-stimulating factor 1 receptor gene results in osteopetrosis, mononuclear phagocyte deficiency, increased primitive progenitor cell frequencies, and reproductive defects. *Blood.* 20002;99:111–120.
29. McKercher SR, Torbett BE, Anderson KL, Henkel GW, Vestal DJ, Baribault H, Klemsz M, Feeney AJ, Wu GE, Paige CJ, Maki RA. Targeted disruption of the PU. 1 gene results in multiple hematopoietic abnormalities. *EMBO J.* 1996;15:5647–5658.
30. Taichman RS. Blood and bone: two tissues whose fates are intertwined to create the hematopoietic stem-cell niche. *Blood.* 2005;105:2631–2639.
31. Matsushita K, Wu Y, Okamoto Y, Pratt RE, Dzau V. Local renin angiotensin expression regulates human mesenchymal stem cells differentiation to adipocytes. *Hypertension.* 2006;48:1095–1102.
32. Kim DH, Yoo KH, Choi KS, Choi J, Choi SY, Yang SE, Yang YS, Im HJ, Kim KH, Jung HL, Sung KW, Koo HH. Gene expression profile of cytokine and growth factor during differentiation of bone marrow-derived mesenchymal stem cell. *Cytokine.* 2005;31:119–126.
33. Shi RZ, Wang JC, Huang SH, Wang XJ, Li QP. Angiotensin II induces vascular endothelial growth factor synthesis in mesenchymal stem cells. *Exp Cell Res.* 2009;315:10–15.

Cancer Immunol Immunother (2009) 58:493–502
DOI 10.1007/s00262-008-0571-9

ORIGINAL ARTICLE

Intravesical administration of γδ T cells successfully prevents the growth of bladder cancer in the murine model

Takeshi Yuasa · Kiyoshi Sato · Eishi Ashihara · Miki Takeuchi · Shinya Maita · Norihiko Tsuchiya · Tomonori Habuchi · Taira Maekawa · Shinya Kimura

Received: 25 March 2008 / Accepted: 22 July 2008 / Published online: 6 August 2008

Abstract
Background Superficial bladder cancers are usually managed with transurethral resection followed by the intravesical administration of Bacillus Calmette-Guerin which requires major histocompatibility complex (MHC) class I expression on cancer cells. Since cancer cells often loose MHC expression, a novel immunotherapy such as MHC-unrestricted γδ T cell therapy is desired.
Objective To clarify the relationship between the expression of MHC class I and clinicopathological features in bladder cancer patients, and investigate the effects of the administration of intravesical γδ T cells on bladder cancer.
Methods Samples from 123 patients who had undergone either transurethral resection or radical cystectomies were examined for MHC expression and the relationship between this and the clinicopathological features was analyzed statistically. The in vitro and in vivo effects of γδ T cells expanded by zoledronic acid (ZOL) against several types of cancer cell line and an orthotopic bladder cancer murine model which was pretreated with ZOL were investigated.
Results MHC-diminished superficial bladder cancer was significantly more progressive than MHC-conservative bladder cancer ($P = 0.047$). In addition, there was a significant association between diminished MHC expression and poor disease free survival ($P = 0.041$) and overall survival ($P = 0.018$) after radical cystectomy. In vitro, all of the cell lines pretreated with 5-μM ZOL showed a marked increase in sensitivity to lysis by γδ T cells. Moreover, intravesical administration of γδ T cells with 5-μM ZOL significantly demonstrated antitumor activity against bladder cancer cells in the orthotopic murine model ($P < 0.001$), resulting in prolonged survival.
Conclusion The present murine model provides a potentially interesting option to develop immunotherapy using γδ T cells for bladder cancer in human.

Keywords Bladder cancer · Intravesical administration · Major histocompatibility complex · γδ T · Zoledronic acid

Abbreviations

BCG	Bacillus Calmette-Guerin
CIs	Confidence intervals
CIS	Carcinoma in situ
^{51}Cr	^{51} Chromium
CTL	Cytotoxic T-lymphocytes.
E/T	Effecter/target cell
IL-2	Interleukin-2
IVIS	In vivo imaging system
HRs	Hazard ratios
Luc	Luciferase
MHC	Major histocompatibility complex
NK	Natural killer
PBMCs	Peripheral blood mononuclear cells
SCID	Severe combined immunodeficiency
siRNA	Small interfering RNA

T. Yuasa and K. Sato contributed equally to the study.

Electronic supplementary material The online version of this article (doi:10.1007/s00262-008-0571-9) contains supplementary material, which is available to authorized users.

T. Yuasa · S. Maita · N. Tsuchiya · T. Habuchi
Department of Urology, Akita University School of Medicine, Akita 010-8543, Japan

K. Sato · E. Ashihara · M. Takeuchi · T. Maekawa · S. Kimura (✉)
Department of Transfusion Medicine and Cell Therapy, Kyoto University Hospital, 54 Kawahara Sakyo-ku, Kyoto 606-8507, Japan
e-mail: shkimu@kuhp.kyoto-u.ac.jp

TUR Transurethral resection
ZOL Zoledronic acid

Introduction

Superficial bladder cancers, which comprise approximately 70% of bladder cancers at initial diagnosis are usually managed with transurethral resection (TUR), followed by the intravesical administration of agents such as mitomycin C, adriamycin, and Bacillus Calmette-Guerin (BCG) [1, 2]. Among these intravesical agents, BCG is considered to be the most effective for the eradication and prophylaxis of recurrent superficial bladder cancer, including carcinoma in situ (CIS) and residual cancers [1–3]. BCG is believed to initially attach to bladder surfaces that are coated with extracellular matrix protein and subsequently cause a local inflammatory reaction in the bladder mucosa, characterized by large numbers of T cells including CD4 positive helper T-lymphocytes, CD8 positive cytotoxic T-lymphocytes (CTL), and macrophages [4]. The CTL-mediated antitumor effect is one of the major contributors of BCG therapy; therefore, preservation of major histocompatibility complex (MHC) class I should be necessary for its efficacy. Indeed, Kitamura et al. [5] recently reported that expression of MHC class I molecules on tumor cells contributes significantly to the therapeutic effect of BCG immunotherapy on bladder cancer. Although information on MHC class I expression patterns in bladder cancer is limited, down-regulation of MHC class I molecules in tumor cells is thought to be an important mechanism of tumor escape from immune surveillance [5, 6].

One of the T-lymphocyte subsets, $\gamma\delta$ T cells, displays MHC-unrestricted cytotoxicity that is reminiscent of natural killer (NK) activity [7, 8]. Currently, $\gamma\delta$ T cells are considered to represent a promising new concept in immunotherapy. Recently, we reported that zoledronic acid (ZOL), the most potent bisphosphonate, induced a significant dose-dependent expansion of $\gamma\delta$ T cells both in vitro and in vivo, mainly to the Vγ 9Vδ 2 subset [9]. These observations have recently facilitated the development of novel auto-immunotherapeutic approaches using in vitro expanded $\gamma\delta$ T cells from patients and have already yielded encouraging preliminary results [10].

In the present study, we attempted to evaluate the use of MHC class I expression as a prognostic factor for bladder cancer and also investigated the use of intravesical $\gamma\delta$ T cells as a possible MHC-unrestricted therapeutic tool against bladder cancer. $\gamma\delta$ T cells, which express many of the NK receptors including inhibitory types that recognize HLA class I such as NK inhibitory receptors (KIR) [11]. This may be advantageous because, the disrupting interactions of KIR with their ligands on tumor cells may enhance antitumor responses mediated by $\gamma\delta$ T cells [12]. In addition, local administration may be more effective in treating cancer compared to systemic administration, owing to a favorable effecter/target cell (E/T) ratio. Indeed, some researchers have succeeded in performing local preclinical immunotherapy using $\gamma\delta$ T cells in subcutaneous and intraperitoneal tumor models [13, 14]. Here, we performed intravesical immunotherapy using a bladder orthotopic model, which is close to the observations in a clinical setting.

Materials and methods

Patients and human samples

All 123 patients underwent either TUR or radical cystectomy and simultaneous bilateral pelvic lymph node dissection at the Department of Urology, Akita University School of Medicine between 1995 and 2003. Samples were fixed in formalin, embedded in paraffin, and sectioned for use in microscopic analysis. Informed consent was provided according to the Declaration of Helsinki. Clinical and pathological data were obtained by retrospective chart review, as previously described [15]. The 1997 TNM classifications were used for tissue staging. Ta is a noninvasive papillary carcinoma and T1 means that the tumor invades sub epithelial connective tissue.

Animals, cell lines, and reagents

Approval for these studies was obtained from the institutional review board at Kyoto University Hospital. Specific pathogen-free 6–8-week-old male Balb/c severe combined immunodeficiency (SCID) mice were used (SLC, Kyoto, Japan). The human bladder cancer cell line UM-UC-3 and KU-7, the small cell lung cancer cell line SBC-5, the non-small lung cancer cell line A549, the fibrosarcoma cell line HT1080, and the mesothelioma cell line 211H were obtained from the American Tissue Type Culture collection (Rockville, MD). ZOL and interleukin-2 (IL-2) were obtained from Novartis Pharma AG (Basel, Switzerland) and Shionogi (Osaka, Japan), respectively. UM-UC-3 cells were stably transfected with the pGL3-control vector (Promega, Madison, WI) and pSV2Neo (the American Type Culture Collection) and denoted as UM-UC-3^{Luc}. These cells were maintained as described previously, to use for the in vivo imaging system (IVIS; Xenogen, Alameda, CA), which detects luciferase (Luc) expression [16]. We confirmed that there was no difference in in vitro proliferation between parental UM-UC-3 and UM-UC-3^{Luc}.

Immunohistochemical staining

Immunohistochemical staining was performed by the conventional avidin–biotin–peroxidase complex method (ABC-Elite, Vector Labs), as described previously [16]. Anti-human MHC-1 monoclonal antibody EMR8-5 (Hokudo, Sapporo, Japan) was used at 1:100 dilution for the evaluation of patients samples. Sections were counterstained with hematoxylin and mounted. Normal mouse IgG was used as a negative control.

Immunohistochemical evaluation

All of the specimens were reviewed independently using light microscopy by investigators who were blind to the clinicopathologic data (TY and NT). Staining results were assessed in a semi-quantitative fashion by two independent investigators, as described previously [5]. Briefly, immunoreactivity for MHC class I was categorized on a scale of 0–3 as follows: 0, undetectable staining; 1, incomplete membrane staining in more than 20% of the tumor cells; 2, moderate to complete staining in the cytoplasm of the tumor cells; 3, complete membrane staining in more than 80% of the tumor cells [5]. MHC class I expression was then classified as negative (scores 0, 1, 2) or positive (score 3) [5].

Western blot analysis

Western blotting analysis was performed as described previously [17]. Equal amounts of protein extracts (50 μg) from peripheral blood mononuclear cells (PBMCs), UM-UC-3 or KU-7 were subjected to 12.5% polyacrylamide gel under denaturing conditions (SDS-PAGE) and then electroblotted onto a PVDF membrane (Millipore, Tokyo, Japan), as described previously [17]. Anti-human MHC-1 monoclonal antibody EMR8-5 with a 1:1,000 dilution was used as the primary antibody. Anti-human vinculin (Abcam, Tokyo, Japan) was used as a loading control.

Human $\gamma\delta$ T cell preparations and culture

Informed consent was obtained for the collection of peripheral blood from healthy volunteers. Human $\gamma\delta$ T cells were prepared as described previously [9]. Briefly, PBMCs were separated individually from blood samples donated from five healthy volunteers using Ficoll-Paque (Pharmacia Biotech, Uppsala, Sweden). PBMCs (1×10^5 cells) were stimulated with 5 μM of ZOL and cultured in 24-well round-bottom microtiter wells (Nunc, Wiesbaden, Germany) for 14 days at 37°C. On days 2, 6 and 10, 50 units/mL IL-2 were added to the culture. These ex vivo expanded $\gamma\delta$ T cells were enriched for the cytotoxicity assay both in vitro and in vivo using a magnetic activated cell sorting system (Miltenyi Biotech, Bergisch Gladbach, Germany) to exclude $\alpha\beta$ T cells, as described previously [9]. After the enrichment, the percentage of $\gamma\delta$ T cells was always more than 99.8% (data not shown).

In vitro cytotoxicity assay

The in vitro cytotoxicity of $\gamma\delta$ T cells from three healthy volunteers against SBC-5, HT-1080, UM-UC-3, 211H, and A549 was examined quantitatively using a standard ^{51}Chromium (^{51}Cr) releasing assay [9]. Briefly, 100-μl aliquots of each cell line that had been pretreated with 5-μM ZOL for 12 h were added to ^{51}Cr for the final 2 h and then washed 3 times. The cells were then incubated for 4 h with ex vivo expanded $\gamma\delta$ T cells at an E/T ratio 10:1, the supernatants were collected, and the radioactivity of ^{51}Cr released from target cells was measured in a gamma counter (Wallac, Gaithersburg, MD). The maximum ^{51}Cr release was determined in target cells treated with Triton X-100 at final concentration of 0.5%. The cytotoxicity was defined as the cell lysis percent according to the formula: cell lysis % = [(experimental release − spontaneous release)/(maximum release − spontaneous release)] × 100.

In vivo effects of $\gamma\delta$ T cells in the orthotopic bladder cancer murine model

In order to establish the orthotopic bladder cancer models, Luc-labeled bladder cancer cells (2×10^6) were implanted into the murine bladder cavity via 24-gauge angiocatheters (Termo, Tokyo, Japan), as described previously [16]. Male BALB/c SCID mice were intravesically administered 1×10^7 UM-UC-3^{Luc} cells. Mice were randomized into four groups: (i) untreated mice, (ii) mice treated with 5-μM ZOL (200 μl), (iii) mice treated with 1×10^7 purified $\gamma\delta$ T cells and (iv) mice treated with 5-μM ZOL (200 μl) and 1×10^7 purified $\gamma\delta$ T cells. Randomization was performed 7 (first experiment) and 3 days (second experiment) after the cancer cell transplantation and each group contained 8 mice. 100 μL of 5-μM ZOL for 3 h and/or 1×10^7 $\gamma\delta$ T cells were administered for 5 sequential days from day 8 to day 12 for the first experiment and from day 4 to day 8 for the second experiment by the transurethral and intravesical method. The effect of $\gamma\delta$ T cells on UM-UC-3^{Luc} was monitored by IVIS (total number of photons), as described previously [18]. To examine how many of the $\gamma\delta$ T cells survive after 3-h incubation in the bladder, 1×10^7 $\gamma\delta$ T cells were administrated by the transurethral and intravesical method to intact bladders. $\gamma\delta$ T cell variability was examined after 3-h incubation in the bladders by the trypan blue dye exclusion method. In addition, to examine how $\gamma\delta$ T cells infiltrate healthy bladder epithelium and/or cancer

lesions, 1×10^7 $\gamma\delta$ T cells were also administrated by the transurethral and intravesical method to orthotopic bladder cancer mice models that had been 21 days earlier inoculated with 1×10^7 UM-UC-3^{Luc} cells. After treatment with ZOL and $\gamma\delta$ T cells, the bladders were dissected (each group, $n = 3$) and examined histologically after hematoxylin–eosin staining and immunohistochemically with anti-human CD3 (Novocastra Laboratories Ltd, Newcastle, UK) by light microscopy.

Statistical analysis

All data were entered into an access database and analyzed using Excel 2000 (Microsoft Co., Tokyo, Japan) and SPSS (version 10.0, SPSS, Inc., Tokyo, Japan) software; a probability (P) of <0.05 was required for statistical significance. Chi-square analysis was used for the variables of sex, age, configuration, grade, stage, and lymphatic and vascular involvement. Recurrence of the superficial cancers was defined as positive cytology or a pathologically proven tumor. Recurrence of invasive cancers was defined as clinically detected tumors, chiefly by imaging. Kaplan–Meier analysis was used to estimate the cumulative recurrence free survival, cause-specific survival, and overall survival rates, and the log-rank test was employed to correlate differences in patient survival with the staining intensity of MHC class I. Hazard ratios (HRs) and 95% confidence intervals (CIs) for disease free survival were assessed by the Cox proportional hazard regression model. The influence of the treatment on the growth of bladder cancers was analyzed by the Student's t test.

Results

Relationship between the expression of MHC class I and clinicopathological features in patients with superficial bladder cancer

We initially tested whether the immunohistochemical levels of MHC class I expression correlated with the clinicopathological features, recurrence and progression free survival of patients with superficial bladder cancer. The histologically high grade, T1, and CIS co-existence bladder cancers demonstrated diminished MHC class I expression which was significantly lower than that in the low grade, Ta, and free of CIS cancer patients (Fig. 1a; Table 1). Moreover, although the difference in recurrence free survival was not significant, patients with low MHC class I expression exhibited a significantly shorter progression free survival than patients with high MHC class I expression (Fig. 1b upper row; $P = 0.047$). In addition, of these patients, 22 underwent BCG instillation therapy. In general, patients with low MHC class I expression had a tendency to exhibit shorter progression free survival than the patients with high MHC class I expression, although this difference

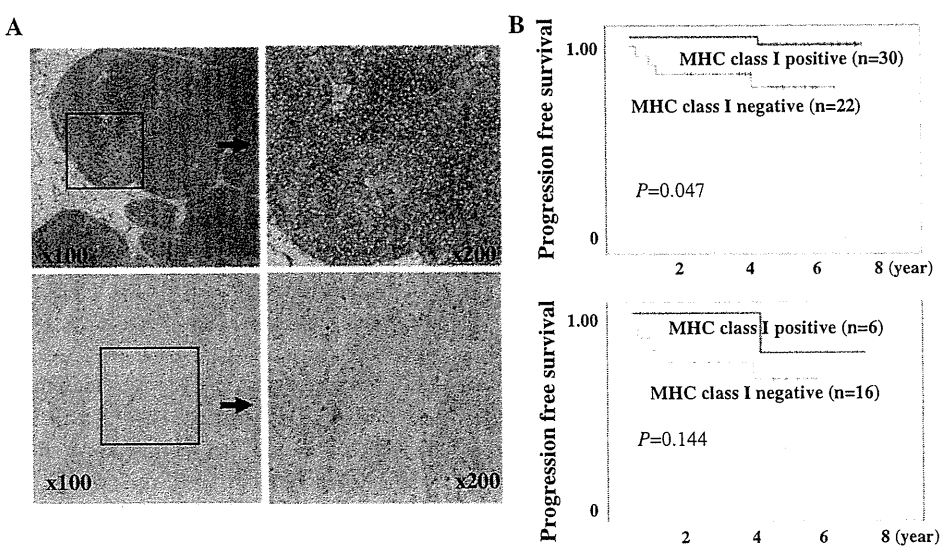

Fig. 1 MHC class I expression correlates with the progression of superficial bladder cancer. **a** MHC class I expression in the tissues of superficial bladder cancer was immunohistochemically analyzed by the conventional avidin–biotin–peroxidase complex method using the anti-human MHC class I monoclonal antibody EMR8-5 at a 1:100 dilution. A strong immune-reaction in low grade bladder cancers (*upper row*) and a weak and diminished immune-reaction in high grade bladder cancers (*lower row*) were typically observed. Nuclear staining was performed with Mayer's hematoxylin. **b** Comparison of the survival curves between patients with bladder cancers expressing high and low levels of MHC class I. Progression free survival curves for patients with superficial bladder cancer (*upper row*) and for those treated with intravesical BCG (*lower row*)

Table 1 Relationship between the level of MHC class I expression and clinicopathological features of the patients with superficial bladder cancer

	Total ($n = 52$)	High ($n = 30$)	Low ($n = 22$)	P value
Age (mean SD)	68.1 (15.4)	67.1 (16.9)	69.4 (13.4)	0.98
Sex				
Male	41	23	18	0.65
Female	11	7	4	
Number of tumors				
CIS	11	3	8	0.50
Solitary	12	7	5	
Multiple	27	20	7	
Grade				
Well/mod	31	23	8	0.0034
Poor	21	7	14	
Depth of invasion				
CIS	11	3	8	0.0013
Ta	27	24	3	
T1	14	3	11	
Recurrence				
Negative	31	18	13	0.95
Positive	21	12	9	
Progression				
Negative	47	29	18	0.072
Positive	5	1	4	
Follow-up in month (mean SD)	43.0 (28.3)	44.9 (31.5)	40.3 (24.5)	0.56

was not statistically significant (Fig. 1b lower row, $P = 0.144$).

Relationship between the expression of MHC class I and clinicopathological features in patients with invasive bladder cancer

Next, we tested whether immunohistochemical levels of MHC class I expression were related to various clinicopathological features and survival rates in patients with invasive bladder cancer. The lymph node involvement and lymphatic invasive bladder cancers demonstrated diminished MHC class I expression by immunohistochemistry, compared to the non-lymph node involvement and non-lymphatic invasive cancers (Fig. 2a; Table 2). Moreover, the patients with low MHC class I expression experienced a significantly shorter disease free survival time and overall survival than patients with high MHC class I expression (Fig. 2b upper and lower row, $P = 0.041$, 0.018, respectively). A Cox proportional hazard regression analysis indicated that perivesical invasion (≥pT3a), high grade, lymph node involvement (pN+), and MHC diminishing were associated with poor disease free survival. However, a multivariate analysis using all of these clinicopathological and molecular factors indicated that only lymph node involvement was a significantly unfavorable prognostic factor independent of other factors ($P = 0.021$). These results suggest that bladder cancers with diminished MHC class I expression are biologically aggressive and treatment-resistant tumors.

Ex vivo-expanded $\gamma\delta$ T cells show cell dose-dependent cytotoxic activity against various cancer cell lines

In order to overcome MHC class I deletion, we investigated the use of $\gamma\delta$ T cells as a potential therapeutic tool. We investigated the cytotoxic activity of ex vivo-expanded $\gamma\delta$ T cells at an E/T ratio of 10:1 against various cancer cell lines. The average cytotoxicity of the $\gamma\delta$ T cells from three healthy volunteers with and without pretreatment of 5 μM of ZOL was 75.2 and 32.4% for SBC-5 small cell lung cancer cells, respectively, 37.3 and 15.9% for HT-1080 fibrosarcoma cells, respectively, 52.2 and 14.8% for UM-UC-3 bladder cancer cells, respectively, 55.0 and 34.2% for 211H mesothelioma cells, respectively, and 30.4 and 13.2% for A549 non-small cell lung cancer cells, respectively (Fig. 3a). The differences in cytotoxicity between cells with no pretreatment and those pretreated with a low dose ZOL were significant for all of the cells examined ($P < 0.001$ for all cells). Thus, $\gamma\delta$ T cells kill various cancer cell lines and a low dose of ZOL can augment their cytotoxic effect.

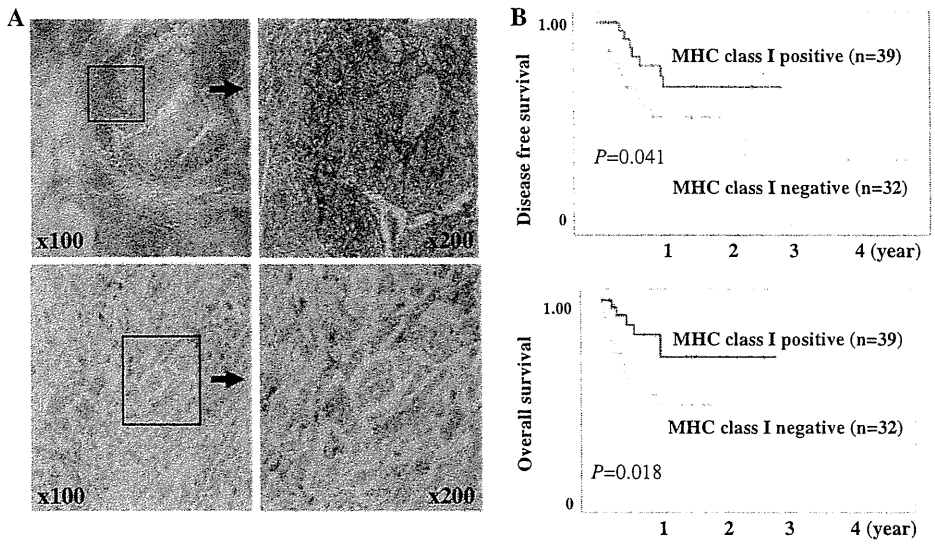

Fig. 2 MHC class I expression correlates with the progression of invasive bladder cancer. **a** MHC class I expression in the tissues of invasive bladder cancer was immunohistochemically analyzed. A strong immune-reaction in moderate grade bladder cancers (*upper row*) and a weak and diminished immune-reaction in high grade bladder cancers (*lower row*) were typically observed. Micropapillary growth pattern of the high grade bladder cancers also demonstrated a diminished immune-reaction (*lower row*). Numbers indicate original magnifications. **b** Comparison of the survival curves between patients with bladder cancers expressing high and low levels of MHC class I. Disease free survival curve (*upper row*) and overall survival curve (*lower row*) for invasive bladder cancer after radical cystectomy

$\gamma\delta$ T cells in the bladder

A total of 86.5 ± 6.3% of $\gamma\delta$ T cells survived after 3-h incubation in the bladder ($n = 5$). UM-UC-3 which was used for in vivo experiments revealed less MHC class I expression than normal human PBMCs and KU-7 cells (Fig. 3b). $\gamma\delta$ T cells massively infiltrated tumor in the bladder, while few $\gamma\delta$ T cells infiltrated the healthy bladder epithelium (Fig. 4a, b). These findings suggested that the treatment of 100 μL of 5-μM ZOL for 3 h and/or 1×10^7 $\gamma\delta$ T cells might show in vivo growth inhibitory effects in the orthotopic murine bladder cancer models.

In vivo growth inhibition of human bladder cancer in orthotopic murine models by transurethral administration of ex vivo-expanded human $\gamma\delta$ T cells

We introduced UM-UC-3^{LUC} cells into the bladder, and observed their bioluminescence by IVIS. Bioluminescence was not detectable the following day, but was faintly detected 3 days later. In the initial experiment (the first experiment), we randomized these mice on day 8 after transplantation and administered the respective intravesical agent for 5 sequential days starting on day 9. There was no difference between these groups, possibly due to a low E/T ratio. In the second experiment, we divided the mice into 4 groups at day 3 after transplantation. We investigated the growth inhibitory effect of the human $\gamma\delta$ T cells with or without a low dose of ZOL (5 μM) in vivo. Figure 4c shows typical images at day 21 taken by IVIS and the growth curves of the respective transplanted cancers in murine bladder (Fig. 4d). Although equivalent numbers of cancer cells were injected, cancer growth rates differed among the treatment groups. Photon emissions from mice treated with both human $\gamma\delta$ T cells and a low dose of ZOL were significantly lower than those from mice in the non-treatment groups ($P < 0.001$). Moreover, the photon emissions from mice treated with human $\gamma\delta$ T cell and a low dose of ZOL were significantly lower than those of the mice from either the $\gamma\delta$ T cells alone or a low dose of ZOL alone ($P = 0.048$, $P < 0.001$, respectively).

The mucosal surfaces of the $\gamma\delta$ T cell treated murine bladders did not show apparent injury and there were no microscopic differences in the non-cancerous bladder mucosa among the treated and non-treatment mice (Fig. 4a). We found no differences in the body weight among the groups of mice. Furthermore, the mice treated with the combination of $\gamma\delta$ T cells and a low dose of ZOL showed apparently better survival compared with the non-treated, $\gamma\delta$ T cell alone or a low dose of ZOL alone treatment groups (Fig. 4e). The median survival time was 31, 58, and 44 days for mice not treated, treated with $\gamma\delta$ T cell alone, and treated with a low dose of ZOL alone, respectively. The median survival time was not reached by mice treated with the combination of $\gamma\delta$ T cell and a low dose of ZOL until the end of the experiment.

A combination of $\gamma\delta$ T cells and a low dose of ZOL inhibited the growth of bladder cancers not only in vitro,

Table 2 Relationship between the level of MHC class I expression and clinicopathological features of the patients with invasive bladder cancer

	Total ($n = 71$)	High ($n = 39$)	Low ($n = 32$)	P value
Age (mean SD)	67.0 (12.6)	67.4 (14.2)	66.4 (11.0)	0.96
Sex				
Male	55	33	22	0.11
Female	16	6	10	
Configuration				
Papillary	14	9	5	0.52
Non-papillary	53	29	24	
Flat	4	1	3	
Number of tumors				
Solitary	24	12	12	0.41
Multiple	43	26	17	
Flat	4	1	3	
Grade				
Well/mod	10	8	2	0.085
Poor	61	31	30	
Depth of invasion				
≤T2	26	15	11	0.72
>T3	45	24	21	
Lymph node involvement				
Negative	18	6	12	0.027
Positive	47	30	17	
Unknown	6	3	3	
Lymphatic invasion				
Negative	31	22	9	0.017
Positive	40	17	23	
Venous invasion				
Negative	41	26	15	0.093
Positive	30	13	17	
Follow-up in month (mean)	28.7 (25.8)	27.3 (20.0)	30.2 (30.2)	0.67

but also in vivo, and the duration of survival was also significantly prolonged by these treatments without any severe adverse effects in the murine model.

Discussion

In this study, we demonstrated that a loss of MHC class I expression in bladder cancer is a poor prognostic factor both for the progression of superficial cancers and the survival of invasive bladder cancers. Approximately 40–90% of human cancers derived from various MHC class I positive tissues have been reported to be MHC class I deficient [6]. Bladder cancers exhibiting a down-regulation of MHC class I expression acquire the ability to escape from T cell-mediated immune responses, consequently resulting in tumor development, progression, and a poor outcome; these observations are in line with other recent reports [5, 6, 19]. Kitamura et al. [5] also clearly show that the expression of MHC class I molecules on bladder cancer cells contributes significantly to the therapeutic effect of BCG immunotherapy and to recurrence free survival of superficial bladder cancer. In contrast, Sharma et al. [20] reported that the presence of intratumoral CD8-positive tumor-infiltrating cytotoxic cells, not MHC class I expression, was significantly associated with clinical outcome among patients with invasive bladder cancer. These controversies might come from the sensitivity of the antibody against human MHC class I. However, their study is also in line with our observation that the CTL-mediated tumor immune microenvironment plays an important role in the tolerance of BCG therapy.

More than 50% of bladder cancers will recur intravesically, and 20–30% of the these cancers will develop to a higher grade and/or stage within the first 5 years of treatment, and progress to local invasive cancers [20]. In order to avoid progression to an invasive cancer, we have investigated the use of small interfering RNA (siRNA) targeting

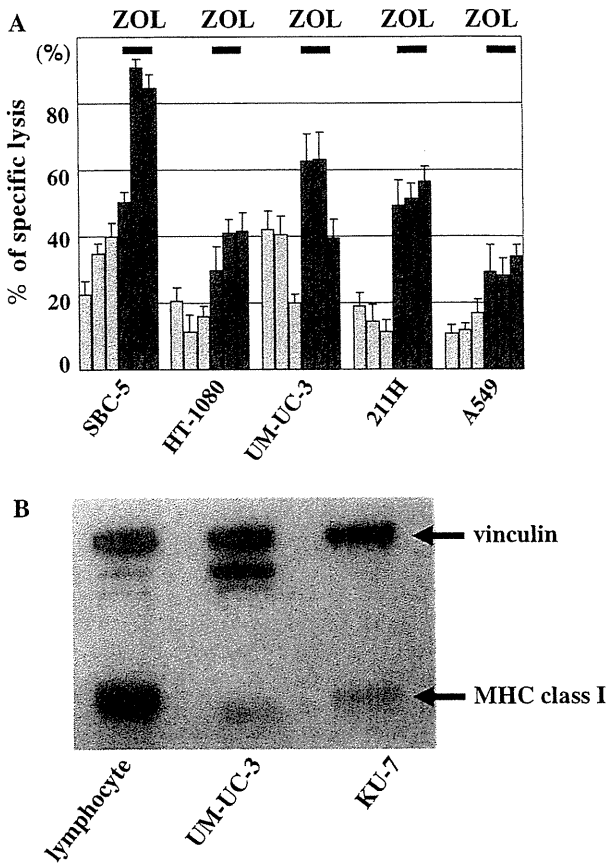

Fig. 3 In vitro combined effects of $\gamma\delta$ T cells with ZOL on various cancer cells and their MHC class I expression. **a** Augmentation of the cytotoxic activity of the ex vivo-expanded $\gamma\delta$ T cells by a low dose of ZOL (5 μM) in various cancer cell lines. In vitro cytotoxicity of $\gamma\delta$ T cells from 3 healthy volunteers against SBC-5, HT-1080 UM-UC-3, 211H, and A549 was examined quantitatively by a standard ^{51}Chromium (^{51}Cr) releasing assay. Each value indicates the mean ± SEM ($n = 6$). **b** MHC class I expressions of human normal PBMNCs, UM-UC-3 and KU-7. The data shown are representative of 3 independent experiments

the *polo like kinase-1 (PLK-1)* gene as a novel therapeutic approach against bladder cancer [16]. We have demonstrated that intravesical administration of *PLK-1* targeted siRNA/cationic liposomes inhibited cancer growth in murine orthotopic bladder cancer models and that the transurethral siRNA therapy could overcome the drug delivery system problem of siRNA delivery.

Molecular targeted therapies are very promising especially for the hematological disorders such as Abl tyrosine kinase inhibitors for chronic myeloid leukemia [21]. However, the efficacy of molecular targeted therapy for solid malignancy remains to be unsolved. A recent topic for urological oncology is the success of sunitinib, which is a novel specific inhibitor of the receptor tyrosine kinases, and anti-angiogenic agents for metastatic renal cell cancer. Although progression free survival was longer and response rates were higher in patients with metastatic renal cell cancer who received sunitinib than in those receiving interferon-α, complete remission was seldom seen even in patients who received sunitinib [22]. The pathogenesis of solid malignancies such as bladder cancer is complicated; therefore, the efficacy of simple gene target therapy is doubtful. We attempted to perform immunotherapy in combination with molecular targeted therapy. We investigated the use of the anti-cancer action of $\gamma\delta$ T cells, which represent a minor subset of human peripheral T cells (1–10%) and contribute to the host immune defense in a different way to CTLs [8].

In this study, we initially demonstrated that $\gamma\delta$ T cells, proliferated by bisphosphonates, demonstrated active anti-cancerous effects against various cancer cells in vitro; this is consistent with previous reports [23]. Kato et al. [23] clearly demonstrated that bladder cancer cells can efficiently present bisphosphonate and pyrophosphomonoester compounds to $\gamma\delta$ T cells, inducing specific proliferation and interferon-γ production. Internalization of bisphosphonates by cancer cells led to rapid inhibition of farnesyl pyrophosphate (FPP) synthase, resulting in intracellular accumulation of isopentenyl pyrophosphate (IPP) upstream of FPP synthase in the mevalonate pathway (Supplemental Fig. 1) [7, 24]. Accumulated IPP acts as a powerful danger signal that activates the immune response and as such might represent a novel target for tumor immunotherapy [7, 9]. We have reported that the tumor killing mechanism of $\gamma\delta$ T cells depends mainly on direct contact involving a perforin-dependent cytolytic pathway [9, 25]. Consequently, we advanced to in vivo experiments.

Here, we have demonstrated that intravesical administration of $\gamma\delta$ T cells with a low dose of ZOL inhibited cancer growth in a murine orthotopic bladder cancer model. Previously, we have confirmed that a high dose of intravesical ZOL resulted in growth inhibition of bladder cancer without any severe side effects [26]. Most current immunotherapeutic approaches such as BCG therapy, which is currently the most effective agent for bladder cancer treatment aim to induce an antitumor response via stimulation of the adaptive immune system, which is dependent on MHC-restricted CTLs. In contrast, $\gamma\delta$ T cells from healthy volunteers, which were proliferated ex vivo, were able to function in an MHC-unrestricted manner and thus, MHC-unrestricted $\gamma\delta$ T cells represent a promising new concept in immunotherapy. The initial failure of the first experiment was probably due to an insufficient E/T ratio; therefore, in the second experiment we administrated $\gamma\delta$ T cells earlier. Improvement of the E/T ratio gave us satisfactory results. Although we have not yet investigated whether patient's $\gamma\delta$ T cells behave similarly as those from healthy volunteers, patient's $\gamma\delta$ T cells might have antitumor effects. Kobayashi

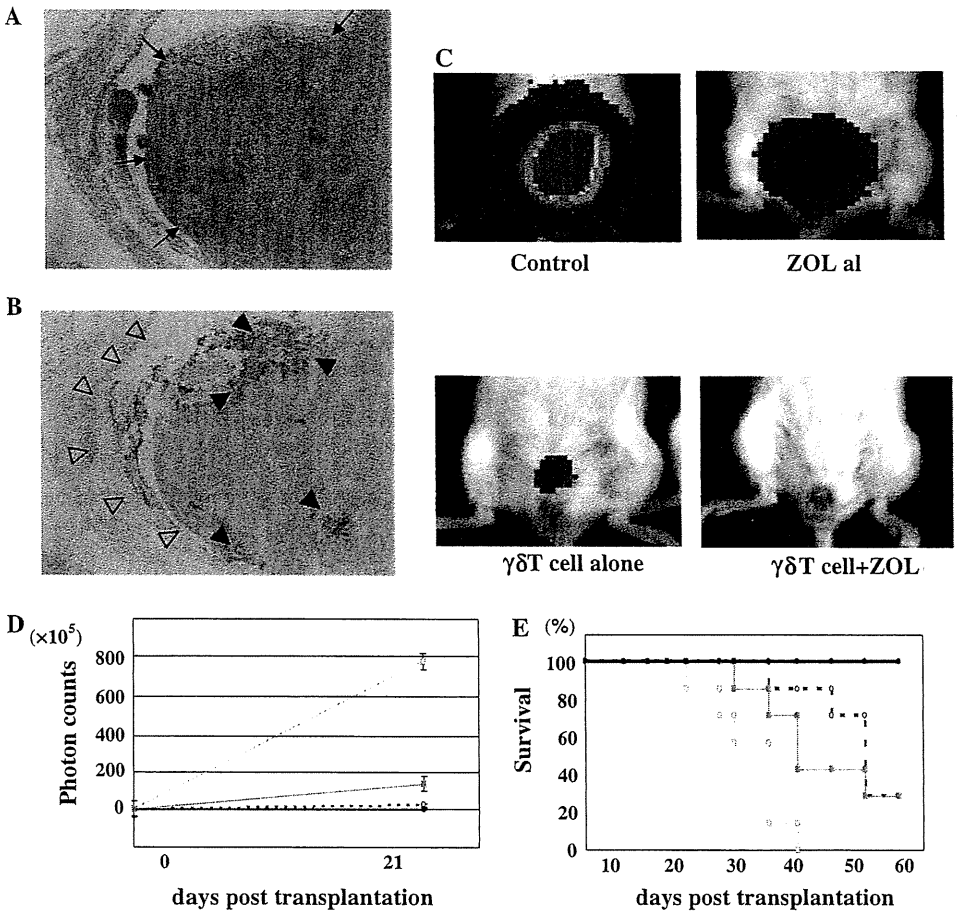

Fig. 4 In vivo effects of intravesical administrated $\gamma\delta$ T cells. After 3-h incubation with ZOL and $\gamma\delta$ T cells, the bladders was occupied by a large tumor (↑) were dissected and examined histologically with hematoxylin-eosine staining (**a**) and immunohistochemically with anti-human CD3 antibody (**b**). Although the region of healthy bladder epithelium (*triangle*) was not infiltrated by $\gamma\delta$ T cells, the tumor was massively infiltrated by $\gamma\delta$ T cells indicated by human CD3 positivity (*filled triangle*). Original magnification ×16. The data shown are representative of 3 independent experiments. **c** In vivo effects of intravesical $\gamma\delta$ T cells in the orthotopic bladder cancer murine model. Typical images of the respective mice not treated or treated with a low dose of ZOL alone, $\gamma\delta$ T cells alone, or $\gamma\delta$ T cells and a low dose of ZOL, were observed by IVIS. **d** The growth curves of orthotopically transplanted UM-UC-3^{LUC} were measured by IVIS. The anti-cancerous effect of intravesical ex vivo-expanded $\gamma\delta$ T cells was demonstrated in vivo: no treatment, *open square*; treatment with a low dose of ZOL alone, *closed square*; treatment with $\gamma\delta$ T cells alone, *open circle*; treatment with $\gamma\delta$ T cells and a low dose of ZOL, closed circle. **e** The survival curves of mice not treated or treated with $\gamma\delta$ T cells alone, a low dose of ZOL alone, or $\gamma\delta$ T cells and a low dose of ZOL. Survival of the orthotopic mice was improved by the intravesical administration of ex vivo-expanded $\gamma\delta$ T cells: no treatment, *open square*; treatment with a low dose of ZOL alone, *closed square*; treatment with $\gamma\delta$ T cells alone, *open circle*; treatment with $\gamma\delta$ T cells and a low dose of ZOL, *closed circle*

et al. [27] reported that adoptive immunotherapy using in vitro-activated autologous $\gamma\delta$ T cells induced antitumor effects in patients with advanced renal cell carcinoma after radical nephrectomy. Taken together, we hypothesize that a combination of molecular targeted therapy such as PLK-1 siRNA and this novel MHC class I-unrestricted immunotherapy may overcome the progression of bladder cancer.

In conclusion, we believe that the antitumor effect of intravesical autologous $\gamma\delta$ T cells is an attractive tool for use as a novel immunotherapy and may cause a breakthrough in clinical applications of cell therapeutics. The efficacy and safety of intravesical $\gamma\delta$ T cells should be verified by early phase clinical trials.

Acknowledgments We thank Ms Yoko Nakagawa, Yoko Mitobe and Yukiko Sugiyama for their skillful technical assistance. This work was partly supported by the Shimadzu Science Foundation, the Sagawa Foundation for Promotion of Cancer Research, Grants-in-Aid for Scientific Research from the Ministry of Education, Culture, Sports, Science and Technology, and the COE program of the Ministry of Education, Culture, Sports, Science and Technology, Japan.

References

1. Jones SJ, Campbell SC (2006) Non-muscle invasive bladder cancer. In: Kavoussi LR, Novick AC, Partin AW, Peters CA, Wein AJ (eds) Campbell-Walsh Urology, 8th edn. Saunders, New York, pp 2447–2467

2. Gee J, Sabichi AL, Grossman HB (2002) Chemoprevention of superficial bladder cancer. Crit Rev Oncol Hematol 43:277–286
3. Herr HW, Laudone VP, Badalament RA, Oettgen HF, Sogani PC, Freedman BD, Melamed MR, Whitmore WF Jr (1988) Bacillus Calmette-Guerin therapy alters the progression of superficial bladder cancer. J Clin Oncol 6:1450–1455
4. Ratliff TL, Ritchey JK, Yuan JJ, Andriole GL, Catalona WJ (1993) T-cell subsets required for intravesical BCG immunotherapy for bladder cancer. J Urol 150:1018–1023
5. Kitamura H, Torigoe T, Honma I, Sato E, Asanuma H, Hirohashi Y, Sato N, Tsukamoto T (2006) Effect of human leukocyte antigen class I expression of tumor cells on outcome of intravesical instillation of bacillus calmette-guerin immunotherapy for bladder cancer. Clin Cancer Res 12:4641–4644
6. Bubenik J (2003) Tumour MHC class I downregulation and immunotherapy. Oncol Rep 10:2005–2008
7. Gober HJ, Kistowska M, Angman L, Jeno P, Mori L, De Libero G (2003) Human T cell receptor gammadelta cells recognize endogenous mevalonate metabolites in tumor cells. J Exp Med 197:163–168
8. Kabelitz D, Wesch D, He W (2007) Perspectives of gammadelta T cells in tumor immunology. Cancer Res 67:5–8
9. Sato K, Kimura S, Segawa H, Yokota A, Matsumoto S, Kuroda J, Nogawa M, Yuasa T, Kiyono Y, Wada H, Maekawa T (2005) Cytotoxic effects of $\gamma\delta$ T cells expanded ex vivo by a third generation bisphosphonate for cancer immunotherapy. Int J Cancer 116:94–99
10. Viey E, Laplace C, Escudier B (2005) Peripheral gammadelta T-lymphocytes as an innovative tool in immunotherapy for metastatic renal cell carcinoma. Expert Rev Anticancer Ther 5:973–986
11. Halary F, Peyrat MA, Champagne E, Lopez-Botet M, Moretta A, Moretta L, Vié H, Fournié JJ, Bonneville M (1997) Control of self-reactive cytotoxic T lymphocytes expressing gamma delta T cell receptors by natural killer inhibitory receptors. Eur J Immunol 27:2812–2821
12. Bakker AB, Phillips JH, Figdor CG, Lanier LL (1998) Killer cell inhibitory receptors for MHC class I molecules regulate lysis of melanoma cells mediated by NK cells, gamma delta T cells, and antigen-specific CTL. J Immunol 160:5239–5245
13. Kabelitz D, Wesch D, Pitters E, Zöller M (2004) Characterization of tumor reactivity of human V gamma 9V delta 2 gamma delta T cells in vitro and in SCID mice in vivo. J Immunol 173:6767–6776
14. Lozupone F, Pende D, Burgio VL, Castelli C, Spada M, Venditti M, Luciani F, Lugini L, Federici C, Ramoni C, Rivoltini L, Parmiani G, Belardelli F, Rivera P, Marcenaro S, Moretta L, Fais S (2004) Effect of human natural killer and gammadelta T cells on the growth of human autologous melanoma xenografts in SCID mice. Cancer Res 64:378–385
15. Ichimura Y, Habuchi T, Tsuchiya N, Wang L, Oyama C, Sato K, Nishiyama H, Ogawa O, Kato T (2004) Increased risk of bladder cancer associated with a glutathione peroxidase 1 codon 198 variant. J Urol 172:728–732
16. Nogawa M, Yuasa T, Kimura S, Tanaka M, Kuroda J, Sato K, Yokota A, Segawa S, Toda Y, Kageyama S, Yoshiki T, Okada Y, Maekawa T (2005) Intravesical administration of small interfering RNA targeting PLK-1 successfully prevents the growth of bladder cancer. J Clin Invest 115:978–985
17. Kimura S, Ito C, Jyoko N, Segawa H, Kuroda J, Okada M, Adachi S, Nakahata T, Yuasa T, Filho VC, Furukawa H, Maekawa T (2005) Inhibition of leukemic cell growth by a novel anti-cancer drug (GUT-70) from *Calophyllim brasiliense* that acts by induction of apoptosis. Int J Cancer 113:158–165
18. Nogawa M, Yuasa T, Kimura S, Kuroda J, Sato K, Segawa H, Yokota A, Maekawa T (2005) Monitoring luciferase-labeled cancer cell growth and metastasis in in vivo models. Cancer Lett 217:243–253
19. Kitamura H, Torigoe T, Honma I, Asanuma H, Nakazawa E, Shimozawa K, Hirohashi Y, Sato E, Sato N, Tsukamoto T (2006) Expression and antigenicity of surviving, an inhibitor of apoptosis family member, in bladder cancer: implications for specific immunotherapy. Urology 67:955–959
20. Sharma P, Shen Y, Wen S, Yamada S, Jungbluth AA, Gnjatic S, Bajorin DF, Reuter VE, Herr H, Old LJ, Sato E (2007) CD8 tumor-infiltrating lymphocytes are predictive of survival in muscle-invasive urothelial carcinoma. Proc Natl Acad Sci USA 104:3967–3972
21. Kimura S, Ashihara E, Maekawa T (2006) New tyrosine kinase inhibitors in the treatment of chronic myeloid leukemia. Curr Pharm Biotechnol 7:371–379
22. Motzer RJ, Hutson TE, Tomczak P, Michaelson MD, Bukowski RM, Rixe O, Oudard S, Negrier S, Szczylik C, Kim ST, Chen I, Bycott PW, Baum CM, Figlin RA (2007) Sunitinib versus interferon alfa in metastatic renal-cell carcinoma. N Engl J Med 356:115–124
23. Kato Y, Tanaka Y, Miyagawa F, Yamashita S, Minato N (2001) Targeting of tumor cells for human gammadelta T cells by nonpeptide antigens. J Immunol 167:5092–5098
24. van Beek E, Pieterman E, Cohen L, Lowik C, Papapoulos S (1999) Farnesyl pyrophosphate synthase is the molecular target of nitrogen-containing bisphosphonates. Biochem Biophys Res Commun 264:108–111
25. Uchida R, Ashihara E, Sato K, Kimura S, Kuroda J, Takeuchi M, Kawata E, Taniguchi K, Okamoto M, Shimura K, Kiyono Y, Shimazaki C, Taniwaki M, Maekawa T (2007) Gamma delta T cells kill myeloma cells by sensing mevalonate metabolites and ICAM-1 molecules on cell surface. Biochem Biophys Res Commun 354:613–618
26. Sato K, Yuasa T, Nogawa M, Kimura S, Segawa H, Yokota A, Maekawa T (2006) A third generation bisphosphonate, minodronic acid (YM529), successfully prevented the growth of bladder cancer in vitro and in vivo. Br J Cancer 95:1354–1361
27. Kobayashi H, Tanaka Y, Yagi J, Osaka Y, Nakazawa H, Uchiyama T, Minato N, Toma H (2007) Safety profile and anti-tumor effects of adoptive immunotherapy using gamma-delta T cells against advanced renal cell carcinoma: a pilot study. Cancer Immunol Immunother 56:469–476

Cancer Letters 274 (2009) 271–278

Contents lists available at ScienceDirect

Cancer Letters

journal homepage: www.elsevier.com/locate/canlet

Clinically relevant dose of zoledronic acid inhibits spontaneous lung metastasis in a murine osteosarcoma model

Kazutaka Koto [a,1], Naoyuki Horie [a,b,1], Shinya Kimura [c,*], Hiroaki Murata [a], Tomoya Sakabe [a], Takaaki Matsui [a], Motonobu Watanabe [d], Souichi Adachi [d], Taira Maekawa [c], Shinji Fushiki [b], Toshikazu Kubo [a]

[a] Department of Orthopedics, Graduate School of Medical Science, Kyoto Prefectural University of Medicine, 465 Kawaramachi-Hirokoji, Kamigyo-ku, Kyoto 602-8566, Japan
[b] Department of Pathology and Applied Neurobiology, Graduate School of Medical Science, Kyoto Prefectural University of Medicine, 465 Kawaramachi-Hirokoji, Kamigyo-ku, Kyoto 602-8566, Japan
[c] Department of Transfusion Medicine and Cell Therapy, Kyoto University Hospital, 54 Kawahara-cho Shogoin, Sakyo-ku, Kyoto 606-8507, Japan
[d] Department of Pediatrics, Kyoto University Hospital, 54 Kawahara-cho Shogoin, Sakyo-ku, Kyoto 606-8507, Japan

ARTICLE INFO

Article history:
Received 8 May 2008
Received in revised form 8 May 2008
Accepted 22 September 2008

Keywords:
Zoledronic acid
Osteosarcoma
Metastasis
Neovascularization

ABSTRACT

Clinically obtainable concentrations of zoledronic acid (ZOL) inhibited the production of vascular endothelial growth factor and reduced the migration, adhesion, and invasiveness of osteosarcoma (OS) cells *in vitro*. The *in vivo* effects of ZOL were investigated by using a murine model of spontaneous lung metastasis. The higher dose of ZOL (80 μg/kg three times/week) inhibited the growth of OS at the primary site, accompanied by inhibition of neovascularization in the tumor. Interestingly, while the lower dose of ZOL (80 μg/kg once a week) could not inhibit the growth of OS at the primary site, it significantly prevented lung metastasis.

1. Introduction

Osteosarcoma (OS) is a high-grade malignant bone neoplasm that occurs primarily in children and adolescents. The prognosis of these patients has improved substantially recently due to the development of various adjuvant and neoadjuvant chemotherapies. However, a significant number still relapse. Recurrence usually occurs as pulmonary metastases or, less frequently, metastases to distant bones or as a local recurrence [1–3]. Thus, a novel strategy that would efficiently inhibit metastasis, especially to the lung, from the primary OS site is highly desirable.

Second- and third-generation bisphosphonates (BPs) were developed primarily to treat benign and malignant bone diseases. They inhibit the proliferation of many kinds of cancer cells by preventing post-translational prenylation of small GTPases such as the Ras family proteins [4]. We reported that third-generation BPs such as zoledronic acid (ZOL) and minodronic acid (YM529) are more directly anti-proliferative *in vitro* than second-generation BPs such as pamidronate [5–8]. Moreover, we also reported that third-generation BPs have direct *in vivo* anti-tumor effects against several cancer cell lines [5–8]. Intriguingly, ZOL also inhibited bone metastasis of breast cancer [9,10] and lung metastasis of OS in mouse models [11].

We are currently focusing on the anti-tumor effects of ZOL against OS cells because we have found that OS cell lines are often more sensitive *in vitro* to ZOL than other cancer cell lines [12,13]. For example, the 50% growth

* Corresponding author. Tel.: +81 75 751 3630; fax: +81 75 751 3631.
E-mail address: shkimu@kuhp.kyoto-u.ac.jp (S. Kimura).
[1] These authors contribute equal to this work.

0304-3835/$ - see front matter © 2008 Elsevier Ireland Ltd. All rights reserved.
doi:10.1016/j.canlet.2008.09.026

inhibitory concentrations (IC_{50}) values of ZOL for the OS cell lines MOS and LM8 were 1.56 μM and 7.36 μM, respectively [13], while those for other cancer cell lines varied from 10 to 60 μM [5–8]. While it remains unclear why OS cell lines are more sensitive to BPs, it may reflect the fact that OS cells usually make osseous or osteoid tissue themselves, which, if mineralized, would increase their propensity to take up BPs [14].

We herein investigated the anti-OS effects of ZOL, including its ability to inhibit metastasis. We first used ZOL *in vitro* at clinically relevant concentrations to determine whether it could directly inhibit the proliferation of the murine OS cell line LM8, which had high lung metastatic potential [15]. The anti-metastatic potential of ZOL was also determined by measuring its *in vitro* ability to inhibit LM8 migration, adhesion, invasion, and production of vascular endothelial growth factor (VEGF). Next, we investigated the *in vivo* anti-tumor effects of ZOL on both primary OS xenografts and metastasis to lung. To do so, we used a mouse model of spontaneous lung metastasis in which mice were inoculated subcutaneously into soft tissue in the lumbar region with LM8 cells that express luciferase. This model was employed because the use of more physiological animal models that closely mimic the human disease would help the translation of preclinical results to the clinic. Ory et al. clearly demonstrated that ZOL inhibited OS lung metastasis [11] but used a mouse model in which OS cells were injected intravenously. Consequently, this model did not reveal the effect of ZOL on the entire spontaneous metastatic process, which involved a number of distinct steps, including invasion, adhesion, migration, intravasation, extravasation, etc. [16,17]. In addition, they used a cumulative dose of ZOL that was higher than the clinically relevant dose. Thus, using an *in vivo* imaging system (IVIS), we investigated the effect of more clinically relevant cumulative doses of ZOL on spontaneous metastasis to the lung after subcutaneous inoculation of OS cells.

2. Materials and methods

2.1. Reagents, cell line, and animals

ZOL [1-hydroxy-2-(1H-imidazole-1-yl)ethylidene-bisphosphonicacid] was supplied as the hydrated disodium salt (molecular weight 401.6) by Novartis Pharma AG (Basel, Switzerland). Geranylgeraniol (GGOH) was obtained from Wako Pure Chemical Co. (Osaka, Japan). Both compounds were used as previously described [18]. The murine OS cell line LM8 was established from the Dunn OS cell line and maintained as described elsewhere [15]. To generate luciferase-expressing LM8 cells ($LM8^{Luc}$), LM8 cells were stably transfected with the pGL3-control vector (Promega, Madison, WI) and pSV2Neo (American Type Culture Collection, Rockville, MD) as previously described [19]. All experiments were performed at least three times. Approval for these studies was obtained from the institutional review board at Kyoto University Hospital. Specific pathogen-free 5- to 6-week-old BALB/c nu/nu mice (Japan Clea, Osaka, Japan) were used. For surgical manipulations, mice were anesthetized by intraperitoneal injection of Nembutal (15 mg/kg body weight) (Abbott Laboratories, North Chicago, IL).

2.2. Proliferation, cell cycle, and protein prenylation

To measure the effect of ZOL on proliferation, LM8 cells were incubated in 12-well plates at 5×10^4 cells/μL for 24 h, after which 2.5, 5.0, or 10 μM of ZOL was added. After 0, 24, 48, or 72 h of further incubation, the viable cells in each well were counted by the trypan blue dye exclusion method. To measure the effect of ZOL on protein prenylation, LM8 cells were incubated in 96-well plates at 2×10^3 cells/μL for 24 h, after which various concentrations of ZOL with or without 10 μM GGOH were added for another 48 h. The cells were then assayed by the methyl-thiazol-diphenyl-tetrazolium (MTT) assay [20]. The means of six values were calculated. The IC_{50} values were calculated with the nonlinear regression program CalcuSyn (Biosoft, Cambridge, United Kingdom). To measure the effect of ZOL on the cell cycle, LM8 cells treated with ZOL for 24 or 48 h were analyzed for cell cycle alterations by propidium iodide (Sigma–Aldrich) staining [21]. The prenylation status of Rap1A, one of Ras family proteins was examined by Western blot analysis using a goat polyclonal anti-Rap1A antibody (diluted 1:1000) (Santa Cruz Biotechnologies, CA) which specifically recognized unprenylated form of Rap1A [5].

2.3. VEGF production

After LM8 cells had been cultured with various concentrations of ZOL for 48 h, the VEGF concentration in each supernatant was determined with an ELIZA assay for murine VEGF (R&D Systems, Minneapolis, MN) according to the manufacturer's instructions.

2.4. Migration, adhesion, and invasion

Non-toxic doses of ZOL were used in conjunction with a 24 h incubation period. Cell migration assays were performed with Bio-Coat cell migration chambers (BD Biosciences, Bedford, MA). LM8 cells were added to the upper chambers at 1×10^5 cells per 100 μL of serum-free medium with or without ZOL, and the chemoattractant (10% FCS) was placed in the lower chamber. As a negative control, serum-free medium was placed in the lower chamber. After 24 h incubation, the cells that had migrated to the membrane surface were fixed with methanol and stained with Giemsa. The membranes were photographed and the cells from 10 random fields (200× magnification) were counted. For adhesion assays, LM8 cells were incubated in collagen type I-coated 96-well plates (IWAKI, Japan) at a density of 2×10^4 cells per well with 0.5, 1.0, and 2.0 μM of ZOL for 24 h. The adherent cells were then counted by using the MTT assay. Cell invasion assays were performed with Bio-Coat cell migration chambers, in which the inserted membranes were coated with Matrigel. LM8 cells were added to the upper chamber at 2×10^5 cells/μL in serum-free medium with or without ZOL, and 10% FCS was placed in the lower chamber. After 24 h, the non-invading cells were removed together with the Matrigel

and the cells that had invaded to the surface of the membrane were fixed with methanol and stained with hematoxylin. The membranes were mounted onto glass slides and the cells from 10 random microscopic fields (200× magnification) were counted.

2.5. Animal model

To generate the spontaneous lung metastasis model, 1×10^7 $LM8^{Luc}$ cells were injected into the subcutaneous soft tissue of the lateral lumbar region. The mice bearing $LM8^{Luc}$ cells were divided into three groups: (i) untreated, (ii) treated with 80 μg/kg ZOL once a week for 4 weeks, and (iii) treated with 80 μg/kg ZOL every day for the first 3 days of the week for 4 weeks. Each group contained 6 mice. ZOL was administered intraperitoneally from day 1 of cell inoculation. After 4 weeks of treatment with ZOL, all mice were killed humanely and their primary tumors and lungs were excised for histological analysis.

Tumor growth at the primary site was monitored by IVIS100 (Xenogen, Alameda, CA) and by measuring tumor volume calculated by the following formula: volume (mm^3) = (smallest diameter)^2 × (largest diameter)/2 as described previously [22]. Briefly, tumor growth at the primary and metastatic site was monitored by IVIS100 with anesthetizing by using isoflurane (Abbott Laboratories). Before mice were anesthetized with isoflurane, an aqueous solution of luciferin (150 mg/kg intraperitoneally) was injected 10 min prior to imaging. The animals were placed into the light-tight chamber of the CCD camera system and the photons emitted from the luciferase-expressing cells within the animal were quantified for 5 min using the software program Living Image (Xenogen) as an overlay on Igor (Wavemetrics, Seattle, WA). Lung metastases were monitored by covering the subcutaneous primary

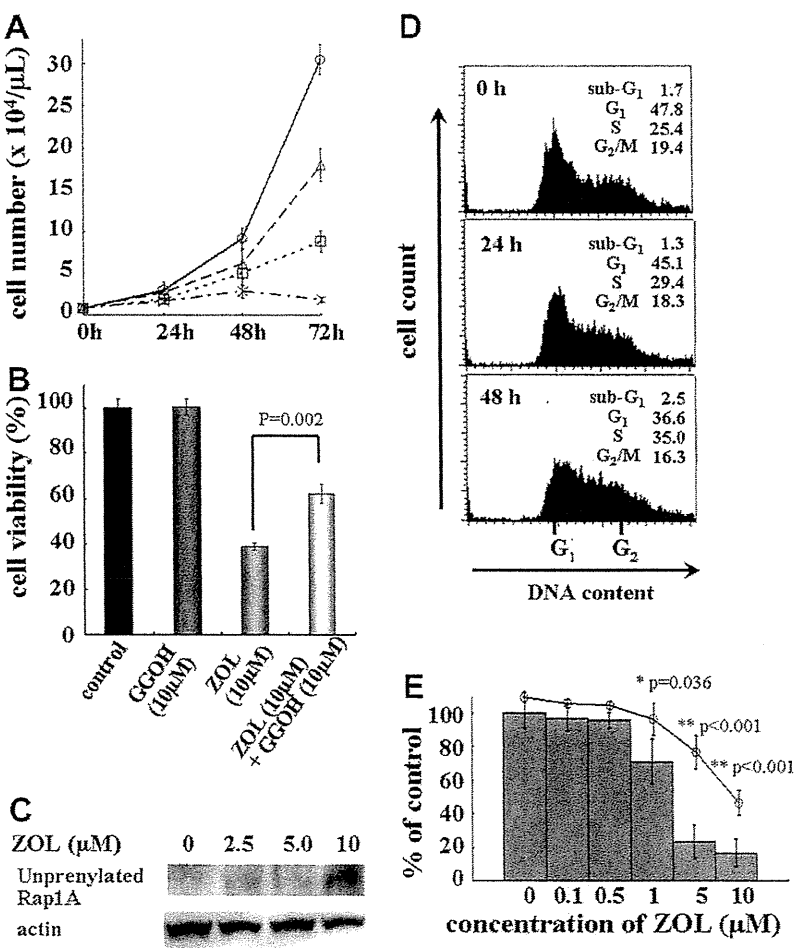

Fig. 1. Effect of ZOL on OS cell proliferation, prenylation and VEGF production. (A) The effect of ZOL on LM8 cell proliferation was determined by the trypan blue dye exclusion method. LM8 cells were exposed to 0 (○), 2.5 (△), 5.0 (□), or 10 μM (×) ZOL. (B) The effect of GGOH on the anti-proliferative ability of ZOL was determined using by the MTT assay. LM8 cells were exposed to 10 μM GGOH and/or 10 μM ZOL for 48 h. (C) LM8 cells were treated with 2.5, 5.0, or 10 μM ZOL for 48 h, after which their lysates were immunoblotted for the unprenylated form of Rap1A. (D) The effect of ZOL on the cell cycle was evaluated by flow cytometric analysis of LM8 cells that had been exposed to 10 μM ZOL for 24 or 48 h. The cell cycle distribution (%) is shown. (E) The effect of ZOL on the release of VEGF from LM8 cells. After 48 h of incubation with various concentrations of ZOL, the culture supernatants were collected and the VEGF concentrations were determined by ELISA (gray bars). The viable cells were also analyzed by using the MTT assay (○). The data are presented as means ± SD of at least three independent experiments.

tumor with a black sheet to prevent the primary site from emitting high levels of photons.

2.6. Histological analysis

Samples were fixed in 10% buffered formaldehyde and then embedded in paraffin. Sections, 4 μM thick, were mounted onto glass slides and stained with hematoxylin–eosin (HE). To determine the number of vascular endothelial cells, immunohistochemical staining was performed with a primary antibody against α smooth muscle actin (SMA) (clone 1A4; Sigma, St. Louis, Missouri, USA). Diaminobenzidine served as a chromogen and the slides were counterstained with hematoxylin. Appropriate positive and negative controls were included in each staining procedure [23]. Ten random microscopic fields (200× magnification) were analyzed with the IP Lab™ software for Apple Macintosh (BD Biosciences).

2.7. Statistics

Results are expressed as mean ± SD. Student's *t*-test was used to determine the statistical significance of detected differences; *p* values were derived from two-sided tests and values less than 0.05 were considered statistically significant.

3. Results

3.1. Effect of ZOL on LM8 cell proliferation and prenylation

ZOL inhibited the growth of LM8 cells in a time- and dose-dependent manner (Fig. 1A). The IC_{50} value of ZOL after 48 h of exposure was 7.36 μM. To determine whether the mevalonate pathway participates in the growth inhibitory effects of ZOL, we examined whether 10 μM GGOH could prevent ZOL from inhibiting the growth of LM8 cells. Indeed, GGOH treatment partially reversed the inhibitory effect of 10 μM ZOL after 48 h, increasing cell viability from 38% to about 61% (Fig. 1B). Western blot analysis of these cells revealed that 10 μM ZOL-treated LM8 cells contained unprenylated Rap1A (Fig. 1C). Flow cytometry of LM8 cells after 24 or 48 h exposure to 10 μM ZOL revealed a decreased frequency of cells in the G_2/M phase and an increased frequency of cells in the S phase (Fig. 1D).

3.2. Effect of ZOL on LM8 VEGF production

To examine whether ZOL affects the angiogenic capability of LM8 cells, we measured the VEGF concentrations in the culture supernatants of ZOL-treated and -untreated LM8 cells. ZOL treatment for 48 h reduced VEGF production in a dose-dependent manner, with 50% reduction being

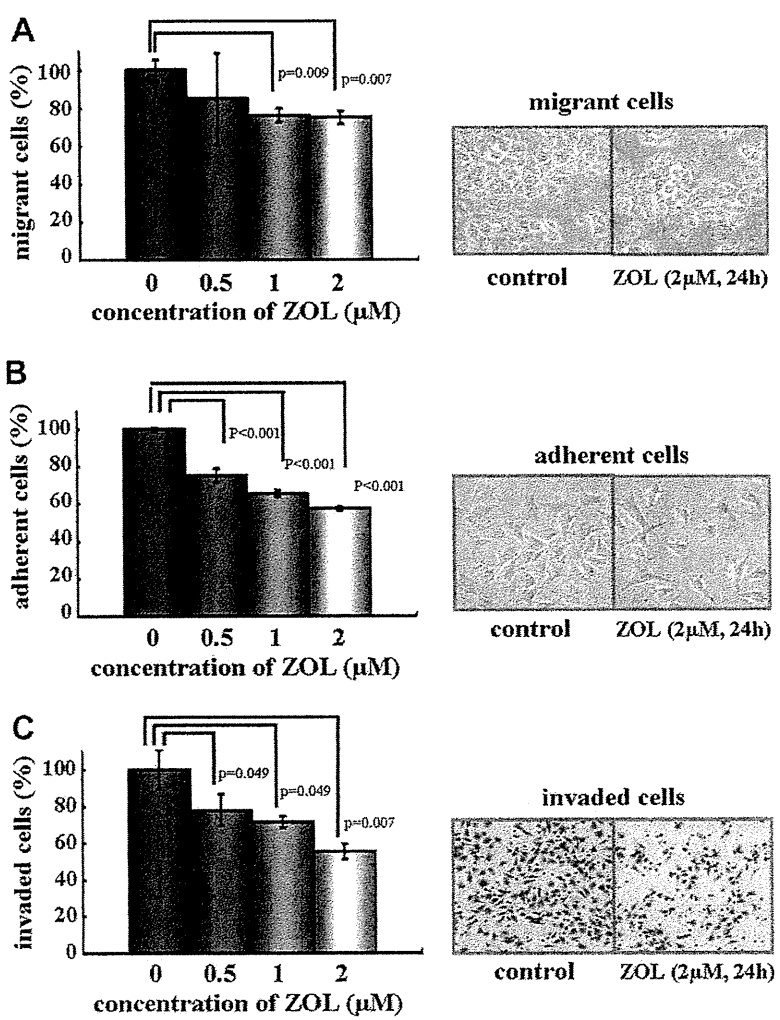

Fig. 2. ZOL prevents the migration, adhesion and invasion of OS cells. The effect of non-toxic doses of ZOL for 24 h on LM8 cell migration (A), adhesion (B) and invasion (C) was analyzed. The data shown are representative of three independent experiments.